

UNIVERSITY OF WARMIA AND MAZURY IN OLSZTYN

# Technical Sciences

**21(3) 2018**



PUBLISHER UWM

## Editorial Board

Ceslovas Aksamitauskas (Vilnius Gediminas Technical University, Lithuania), Olivier Bock (Institut National de L'Information Géographique et Forestière, France), Stefan Cenkowski (University of Manitoba, Canada), Adam Chrzanowski (University of New Brunswick, Canada), Davide Ciucci (University of Milan-Bicocca, Italy), Sakamon Devahastin (King Mongkut's University of Technology Thonburi in Bangkok, Thailand), German Efremov (Moscow Open State University, Russia), Mariusz Figurski (Military University of Technology, Poland), Maorong Ge (Helmholtz-Zentrum Potsdam Deutsches GeoForschungsZentrum, Germany), Dorota Grejner-Brzezinska (The Ohio State University, USA), Janusz Laskowski (University of Life Sciences in Lublin, Poland), Arnold Norkus (Vilnius Gediminas Technical University, Lithuania), Stanisław Pabis (Warsaw University of Life Sciences-SGGW, Poland), Lech Tadeusz Polkowski (Polish-Japanese Institute of Information Technology, Poland), Arris Tijsseling (Technische Universiteit Eindhoven, Netherlands), Vladimir Tilipalov (Kaliningrad State Technical University, Russia), Alojzy Wasilewski (Koszalin University of Technology,

## Poland) Editorial Committee

Marek Markowski (Editor-in-Chief), Piotr Artiemjew, Kamil Kowalczyk, Wojciech Sobieski, Piotr Srokosz, Magdalena Zielińska (Assistant Editor), Marcin Zieliński

## Features Editors

Piotr Artiemjew (Information Technology), Marcin Dębowski (Environmental Engineering), Zdzisław Kaliniewicz (Biosystems Engineering), Grzegorz Królczyk (Materials Engineering), Marek Mróz (Geodesy and Cartography), Ryszard Myhan (Safety Engineering), Wojciech Sobieski (Mechanical Engineering), Piotr Srokosz (Civil Engineering), Jędrzej Trajer (Production Engineering)

## Statistical Editor

Paweł Drozda

## Executive Editor

Mariola Jezierska

The Technical Sciences is indexed and abstracted in BazTech (<http://baztech.icm.edu.pl>) and in IC Journal Master List (<http://journals.indexcopernicus.com>)

The Journal is available in electronic form on the web sites  
<http://www.uwm.edu.pl/techsci> (subpage Issues)  
<http://wydawnictwo.uwm.edu.pl> (subpage Czytelnia)

The electronic edition is the primary version of the Journal

PL ISSN 1505-4675

e-ISSN 2083-4527

© Copyright by Wydawnictwo UWM • Olsztyn 2018

## Address

ul. Jana Heweliusza 14  
10-718 Olsztyn-Kortowo, Poland  
tel.: +48 89 523 36 61  
fax: +48 89 523 34 38  
e-mail: [wydawca@uwm.edu.pl](mailto:wydawca@uwm.edu.pl)

## Contents

A. GRZYBOWSKA, Ł. MROZIK – <i>Use of Admixture Effectiveness Curves for Prediction of the Compressive Strength of Concrete</i> .....	175
A. SZEGDA, S. RADKOWSKI, S. BROL – <i>Magnetic Field of a Radial Tire after Puncture Caused by Ferromagnetic Elements</i> .....	183
I. TRAWCZYŃSKA, J. MILEK, S. KWIATKOWSKA-MARKS – <i>Effect of Temperature, Concentration of Alcohols and Time on Baker's Yeast Permeabilization Process</i> .....	195
M. MAŁEK, W. ŻYCIŃSKI, M. JACKOWSKI, M. WACHOWSKI – <i>Effect of Polypropylene Fiber Addition on Mechanical Properties of Concrete Based on Portland Cement</i> .....	207
J. JAROSZEWICZ, K. ŁUKASZEWICZ – <i>Analysis of Natural Frequency of Flexural Vibrations of a Single-Span Beam with the Consideration of Timoshenko Effect</i> .....	215
M. PAŃTAK, K. MARECIK – <i>Assessment of Comfort of Use of Footbridges ...</i>	233





## USE OF ADMIXTURE EFFECTIVENESS CURVES FOR PREDICTION OF THE COMPRESSIVE STRENGTH OF CONCRETE

*Agnieszka Grzybowska, Łukasz Mroził*

Faculty of Civil and Environmental Engineering and Architecture  
University of Science and Technology, Bydgoszcz

Received 5 May 2017; accepted 22 May 2018; available online 12 June 2018.

**Key words:** additive, cement paste, low water-binder ratio, effectiveness curve.

### Abstract

This paper presents the results of individual laboratory tests conducted in the Research and Experiment Facility of the University of Science and Technology in Bydgoszcz, in particular of tests conducted on pastes of low water-binder ratios (from 0.2 to standard water demand (MROZIŁ 2012)). The purpose of this document is to examine the effect of the applied admixtures (plasticizer or superplasticizer) and its amount on the bulk density of a cement paste, thus on the compressive strength of concrete (as shown in the paper (NEVILLE 2012), properties of concrete can be estimated on the basis of pastes). Conclusions concerning the suitability of specific amounts of plasticisers and superplasticizers were formulated and effectiveness curves were established on the basis thereof.

### Introduction

High performance concrete provides many more opportunities as compared with ordinary concrete. However, their production requires the use of high class cement, aggregate of appropriate quality and quantity, chemical admixtures and special methods of compacting (AİTCIN 2014, BENTZ, CONTWAY 2001, CZARNECKI, JUSTNES, 2012, MROZIŁ 2012, NEVILLE 2012. It is also important to obtain a low water-binder ratio which ensures that concrete is less porous, its absorption properties are reduced, while frost resistance improves. In particular, its

---

Correspondence: Agnieszka Grzybowska, Katedra Konstrukcji Budowlanych, Wydział Budownictwa, Architektury i Inżynierii Środowiska, Uniwersytet Technologiczno-Przyrodniczy w Bydgoszczy, al. Prof. S. Kaliskiego 7, 85-769 Bydgoszcz, e-mail: grzybowska.utp@gmail.com

compressive strength increases (which is one of the components of high performance concrete properties). A low value of the water-binder ratio causes problems with concrete mixture workability, therefore it is necessary to use plasticizers or superplasticizers (BENTZ, CONTWAY 2001, CHEN et al. 2013, ŁUKOWSKI 1998). As is known, the bulk density of a paste, which is the weight-to-volume ratio, together with binder (cement) air void has a direct impact on the compressive strength of a finished cement composite (BHANJA, SENGUPTA 2003, MROZIK 2012, NEVILLE 2012). This was a basis for considerations of this subject matter. The purpose of this paper is to present the results of tests of the influence of selected admixtures (plasticizers or superplasticizers) and their amounts on the bulk density of a cement paste. Effectiveness curves of the additives were developed to determine their effective share in the mixture. Conclusions concerning the strength of high performance concrete produced with low water-binder ratio pastes were formulated on the basis thereof.

## Material and methods

Laboratory tests of cement pastes were conducted with the following admixtures:

- plasticizer no. 1 (a chemical admixtures of the new generation produced on the basis of modified lignosulphonates; owing to a greasing effect, it reduces the amount of batched water at consistent texture and improves the fluidity and cohesion of a concrete mixture at a constant value of the water-cement ratio);
- superplasticizer no. 2 (a chemical admixtures of the new generation produced on the basis of modified polycarboxylates; it reduces the amount of batched water through a greasing and steric effect and causes disaggregation of binder grains, which ensures production of concrete of a very low water-cement ratio).

Cements of the following classes were applied: CEM I 42.5 R (Portland, rapid hardening), CEM IV/B(V) 32.5 R – LH/NA (pozzolanic, rapid hardening with siliceous fly ash (up to 10%), low-alkaline of low hydration heat), CEM II/A-M (S-LL) 52.5 N (mixed Portland, normal hardening, containing furnace slag and limestone – the amount of the above-mentioned additives should fall within the range of 36–55% and the content of silica fume must not exceed 10%). 42.5 R cement is a basis, the composition of which is not modified by mineral additives. Results may be reproducible due to their lower distribution in comparison with the results obtained with different batches of multi-component cement. Portland cements are characterised by a very high hydration heat, rapid strength growth and slightly longer curing time. The basic difference between Pozzolanic cement properties, in particular between the analysed CEM IV/B and Portland cements, is that they are characterised by a slower hardening rate resulting from a low pozzolanic reaction rate, extended setting time and higher resistance

to chemically aggressive factors. The above multi-component cement was taken for tests due to significant differences between respective binder water demands. Tests of cement pastes were carried out, since concrete properties can be estimated on the basis of pastes, as shown in the paper (Neville, 2012). The tests were conducted on the following pastes: without admixtures, with admixture no. 2 in the amount of 0.8%, 3% and 6% (for CEM I) and with admixture no. 1 in the amount of 0.5%. Samples were made with water-binder ratios from 0.15-0.50 and weighed after compacting on a vibration table. 102 samples (for each type of cement) were made in total. They had different components and a water-binder ratio which for pastes without admixtures and including admixture no. 1 was: 0.21, 0.24, 0.27, 0.30, 0.33, 0.36, 0.40, 0.45 and 0.50, whereas for pastes with admixture no. 2, additional samples of 0.15 and 0.18 ratio were prepared. The samples were made in cylindrical moulds of a known volume of 208 cm<sup>3</sup>, repeating the test three times for each water-binder ratio.

## Results and discussion

The obtained results of the density of pastes without admixtures and including admixture no. 2 in the following quantities: 0.8%, 3% (for CEM II and CEM IV) and 0.8%, 3% and 6% (for CEM I) were compared and shown in Figures 1, 3 and 6. A similar list was made for a paste without admixtures and including admixture no. 1 in the amount of 0.5% and shown in Figures 2, 4 and 6.

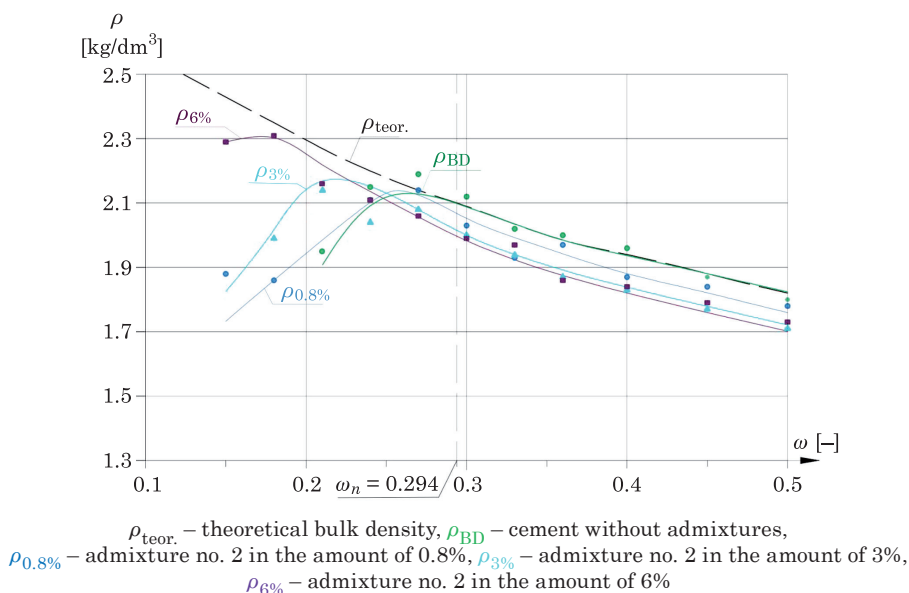


Fig. 1. Bulk density of pastes with superplasticizer no. 2 for CEM I

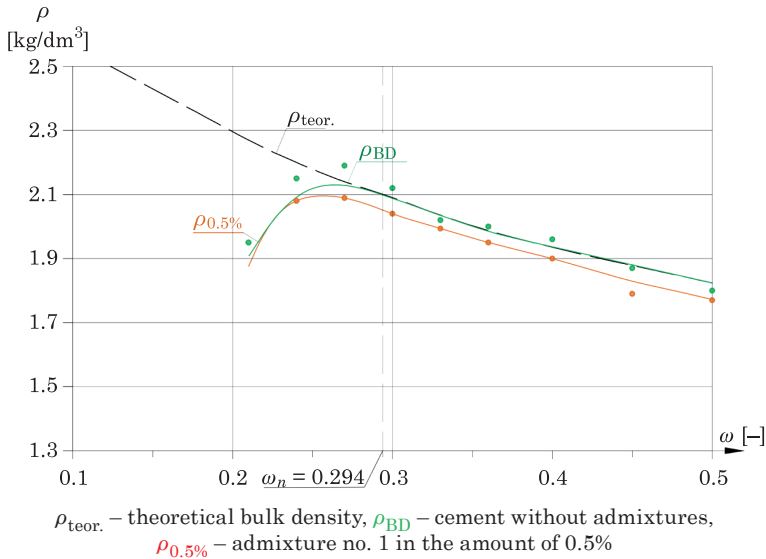


Fig. 2. Bulk density of pastes with plasticizer no. 1 for CEM I

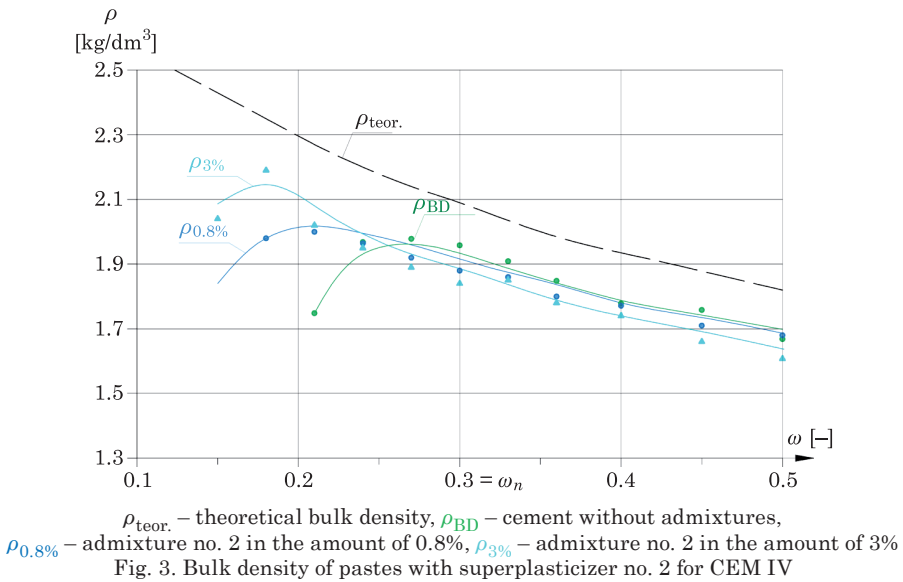
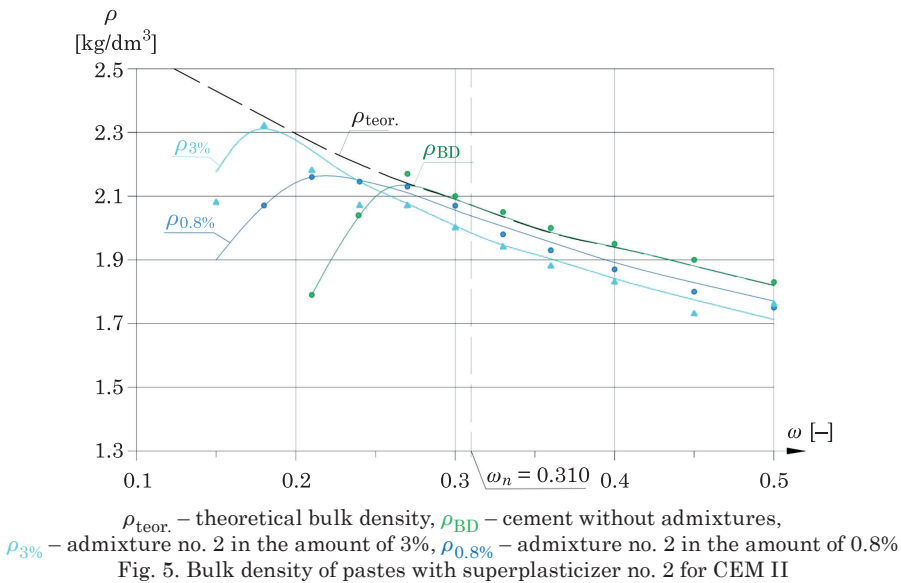
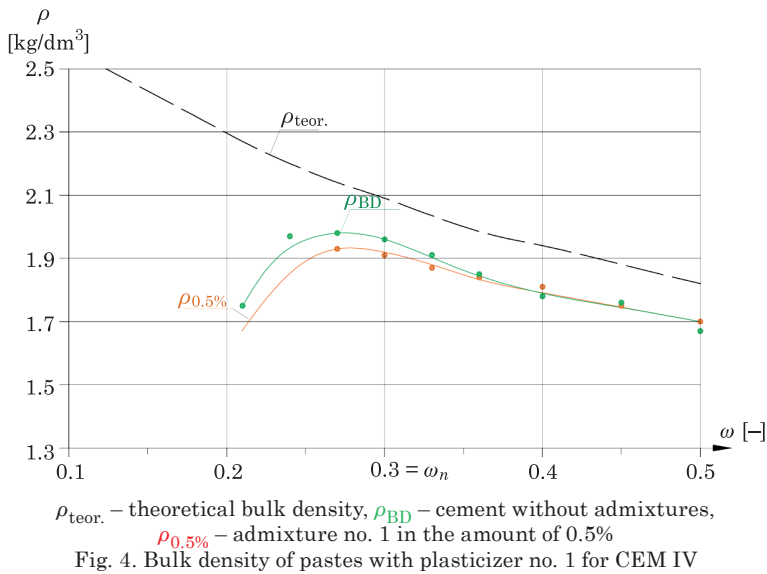


Fig. 3. Bulk density of pastes with superplasticizer no. 2 for CEM IV

It should be emphasized that new generation additives no. 2 have a particularly strong influence on the bulk density due to their electrostatic and steric effect, whereas additive no. 1 has little influence. Moreover, the relations shows an obvious impact of the quantity of the applied admixture on the analysed properties. The above vertical translation of the charts with regard to





the theoretical density calculated on the basis of a water-binder ratio for the amounts of water greater than that resulting from the standard water demand indicates air-entraining properties of admixtures.

Empirical relations between the quantitative and qualitative shares of an admixture which reduces the amount of batched water and the bulk density

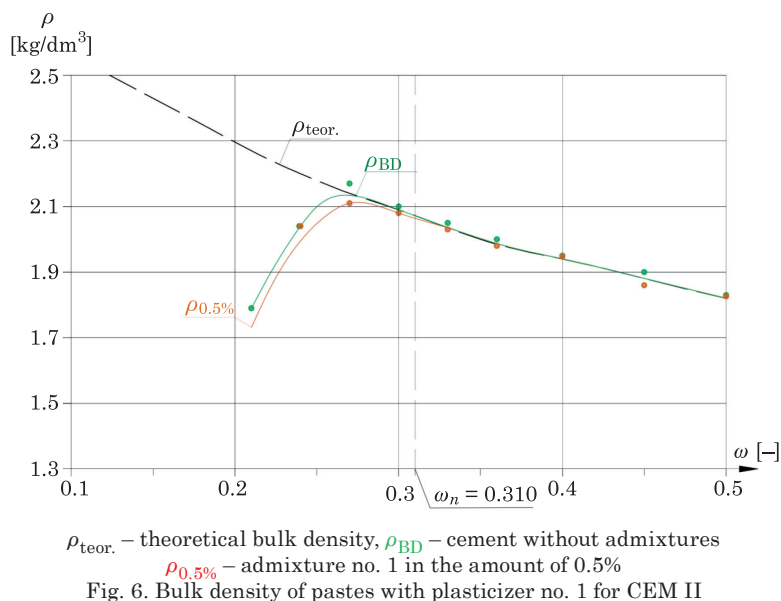


Fig. 6. Bulk density of pastes with plasticizer no. 1 for CEM II

of a paste provide a practical opportunity to design concrete of extremely low water-binder ratios. It is commonly known that the most favourable structure of a cement stone is obtained at extremely reduced share of batched water. It is not enough though, since at low values of the water-binder ratio the necessity to maintain proper workability constitutes a problem. Insufficient workability makes compacting of a paste or concrete mixture much harder, which results in the presence of scattered mesopores and macropores decreasing the strength and impairing other essential properties (absorption, frost resistance, etc.). Taking this into consideration, the compressive strength prediction cannot be based on the water-binder ratio and the quantitative and qualitative share of composites. The paper (MROZIK 2012) shows that there is a minimum amount of water for each paste at which it is possible to obtain the highest bulk density of the paste. At the same time, the greatest volume fraction of binder grains is obtained with this share. For a paste without admixtures, this quantity is similar to that resulting from the standard water demand of the binder, while for plasticizer and superplasticizer modified pastes it results from the quantitative and qualitative share of the admixture. Therefore, designing concrete of extremely low water-binder ratios should be based on experimental tests.

A simplified equation of the high performance concrete strength was applied in the paper (MROZIK 2012):

$$f_{cm} = \alpha_g \cdot R_c \cdot \frac{\sqrt[3]{1 + 0,5 \cdot \frac{\rho_c}{\rho_w} - 1}}{\sqrt[3]{1 + \omega \cdot \frac{\rho_c}{\rho_w} - 1}},$$

where:

- $\omega$  – a water-binder ratio [-],
- $\rho_w$  – density of water [kg/m<sup>3</sup>],
- $\rho_c$  – density of cement [kg/m<sup>3</sup>] (it can be taken as equal to 3,100 kg/m<sup>3</sup>),
- $\alpha_g$  – a ratio including the effect of coarse aggregate on the concrete strength [-], for crushed-stone aggregate  $\alpha_g = 1.3-1.4$ ,
- $R_c$  – cement strength class [MPa].

On the basis of the above relation, a theoretical maximum strength of high performance concrete was estimated with the following assumptions:

- no addition of micro-fillers,
- vibration compacting,
- no thermal and pressure treatment,
- use of coarse aggregate of good quality ( $\alpha_g = 1.4$ ),

The value of the water-binder ratio  $\omega_{opt}$  was used for the above formula, at which the highest apparent density of a paste with identical components was obtained. The results are shown in the Table 1.

Table 1

Maximum theoretical strength of high performance concrete

No.	Paste	$\omega_{opt}$ [-]	$f_{cm}$ [MPa]
1	CEM I 42.5 R without admixtures	0.265	98.5
2	CEM I 42.5 + admixture no. 2 in the amount of 0.8%	0.258	100.7
3	CEM I 42.5 + admixture no. 2 in the amount of 3%	0.220	115.1
4	CEM I 42.5 + admixture no. 2 in the amount of 6%	0.180	136.8
5	CEM I 42.5 + admixture no. 1 in the amount of 0.5%	0.253	102.3
6	CEM IV 32.5 R without admixtures	0.265	75.3
7	CEM IV 32.5 R + admixture no. 2 in the amount of 0.8%	0.208	92.3
8	CEM IV 32.5 R + admixture no. 2 in the amount of 3%	0.180	104.6
9	CEM IV 32.5 R + admixture no. 1 in the amount of 0.5%	0.265	75.3
10	CEM II 52.5 N without admixtures	0.265	121.6
11	CEM II 52.5 N + admixture no. 2 in the amount of 0.8%	0.215	145.0
12	CEM II 52.5 N + admixture no. 2 in the amount of 3%	0.178	170.6
13	CEM II 52.5 N + admixture no. 1 in the amount of 0.5%	0.270	119.8

## Conclusions

Production of concrete of low water-binder ratios requires chemical admixtures which reduce the amount of batched water (ŁUKOWSKI 1998). However, it is difficult to select admixtures (PN-EN 934-1:2009) for concrete of assumed strength parameters in proper quantities and quality. This refers in particular to the analysed group of composites of a low relative water content in the mixture. There are no universal criteria for assessing the effectiveness of binder-admixture sets with regard to the improvement of workability of mixtures made of water in the amount lower than that resulting from the standard water demand of the binder. The proposition of the authors of this paper is to use the above effectiveness curves. They can be used to estimate a minimum value of a water-binder ratio at which effective compacting at a specific amount of an admixture is possible. This value corresponds to the maximum possible compressive strength which can be calculated on the basis of commonly known relations which are deemed precise. Thus, effectiveness curves can be used by technologists to resolve problems such as selection of an effective admixture for high performance concrete of a specific water-binder ratio.

## Literature

- AİTCİN P.C. 2014. *The problems with high strength and low w/c ratio concretes*. Cement Wapno Beton, 2: 127-137.
- BENTZ D.P., CONTWAY J.T. 2001. *Computer modeling of the replacement of "coarse" cement particles by inert fillers in low w/c ratio concretes*. Cement and Concrete Research, 31: 503-506.
- BHANJA S., SENGUPTA B. 2003. *Modified water-cement ratio law for silica fume concretes*. Cement and Concrete Research, 33(03): 447-450.
- CHEN H., WYRZYKOWSKI M., SCRIVENER K., LURA P. 2013. *Prediction of self - desiccation in low water - to-cement ratio pastes based on pore structure evolution*. Cement and Concrete Research, 49: 38-47.
- CZARNECKI L., JUSTNES H. 2012. *Zrównoważony, trwały beton*. Cement Wapno Beton, 6: 341-362.
- ŁUKOWSKI P. 1998. *Domieszki chemiczne do zapraw i betonów*. Wydawnictwo Polski Cement, Kraków.
- MROZIK Ł. 2012. *Model struktury i wytrzymałość betonu wysokowartościowego*. Uniwersytet Technologiczno-Przyrodniczy, Bydgoszcz.
- NEVILLE A.M. 2012. *Właściwości betonu*. Stowarzyszenie Producentów Cementu, Kraków.
- PN-EN 934-1. 2009. *Domieszki do betonu, zaprawy i zaczynu*. Część 1. *Wymagania podstawowe*.



## MAGNETIC FIELD OF A RADIAL TIRE AFTER PUNCTURE CAUSED BY FERROMAGNETIC ELEMENTS

*Agnieszka Szegda*<sup>1</sup>, *Stanisław Radkowski*<sup>2</sup>, *Sebastian Brol*<sup>1</sup>

<sup>1</sup>Department of Vehicles, Faculty of Mechanical Engineering  
Opole University of Technology

<sup>2</sup>Institute of Vehicles, Faculty of Automotive and Construction Machinery Engineering  
Warsaw University of Technology

Received 14 November 2017; accepted 23 May 2018; available online 12 June 2018.

**Key words:** magnetic profile, tire, ferromagnetic penetrator.

### Abstract

Tire, an element of wheel, is made in a sophisticated vulcanization process of many components and some of which such as: bead wire, belt and carcass exhibit ferromagnetic properties. Such components create variable in direction and intensity magnetic field, which expands around tire and the complete wheel. Since the layout of magnetic field is exceptional for every single wheel many of information might be obtained on the basis of it alteration. The reported since now application concentrates on rotational speed measurement, wheel rotations counting and therefore also vehicle linear speed and distance estimation. However up to the present the known solutions did not describe changes in magnetic field in case of damage induced by e.g. puncture caused by ferromagnetic elements. This paper's aim is to test the thesis that it is possible to detect puncture in tire made by ferromagnetic element by using measurement and analysis of changes of magnetic flux density around tire. The tests were executed using original measuring device, designed especially for such experiments. It registers a magnetic profile, which consists of data series of magnetic flux density measured in this investigations 55 mm above tire's tread and arranged along with rotation angle. Tire magnetic properties were assessed by using of circumferential magnetic profiles and parameters such as: minimum value ( $M_{\min}$ ), maximum value ( $M_{\max}$ ), peak to peak value ( $M_m$ ), average value of ordinates of profile ( $M_b$ ), skewness of ordinate distribution ( $M_s$ ) and kurtosis of ordinate distribution ( $M_k$ ). Magnetic profiles before after puncture were analysed as well as the parameters. Moreover differential signal caused by puncture were determined. It turned out that detected changes are directly related to tire damage and showing in rotation angle where puncture occurs.

Correspondence: Sebastian Brol, Katedra Pojazdów, Politechnika Opolska, ul. Mikołajczyka 5, 45-271 Opole, e-mail: [s.brol@po.opole.pl](mailto:s.brol@po.opole.pl)

## Introduction

Monitoring condition of tires in the context of detecting a potential tire's puncture is important for road traffic safety. Tire puncture could lead to diminishing tire pressure which may affect car stability and control. The rate of pressure changes is a separate aspect. It could be slow, when driver has time to react and counteract to effects of fall in tire pressure unless the fall is rapid which frequently ends in a serious damage to wheel, vehicle or other vehicles in traffic. Because of that modern vehicle has been endowed in systems diagnosing selected wheel parameters. An example of such a system is TPMS (Tire Pressure Monitoring System). This solution can be direct or indirect. Indirect system (monitoring) detects difference in dynamic radius of the wheel in car and on this basis indicates which tire in vehicle has lost pressure. Direct system (diagnosing) determines a state of a wheel on the basis of pressure measured in a tire.

Car tire is a complex element created in a multi-stage process. Some components of a tire i.e. bead wire or carcass have ferromagnetic properties and their magnetic field can be measured with resistomagnetic sensors (GONTARZ, RADKOWSKI 2011, CHMIELEWSKI et al. 2011, BROL, SZEGDA 2017). Changes in the magnetic field created due to puncture of a tire with a ferromagnetic penetrator might constitute a basis for wheel diagnosis.

In previous research of the magnetic field around a wheel the focus was mainly directed on examining the influence of low frequency changes in magnetic flux density on human health. In the position by (JENS 2002) the distribution and strength of the magnetic field in different vehicles were compared. Magnetic flux density value was measured in eight points of the vehicle when the engine was running and, e.g. running alternator, fuel pump and other devices in a car that generate magnetic field. The measurement was made using TriField meter by Alpha Labs. The researchers in investigation determined a EMF distribution (Electromagnetic Field) at driver's seat. In the article (GAJŠEK et al. 2010) it was also claimed that hybrid cars have stronger magnetic field than cars with traditional diesel or gasoline engines. In the works MILHAM et al. (1999) and STANKOWSKI et al. (2003) an influence of low frequency changes in the magnetic field of radial tire on human health was examined as well as distribution of the field in a car. By using fluxgate magnetometer (Walker FGM-301) and a simple magnetic compass (R.B. Annis Company, Magnetic Equipment) changes of the magnetic field in both new and old tires were examined. The researchers carried out research on radial tires before and after demagnetization. They concluded that a magnetic field value is directly related with magnetism of a steel wire used in tire. In the paper the researchers have also analyzed changes in tire magnetic field by magnetizing and demagnetizing it in a controlled way. The magnetic field was registered by NARDA EFA200 Electro-magnetic Field Analyzer together with a BN2245/90.10 field probe (Telemeter

Electronic, Ellighausen, Germany). The results confirmed that tire magnetism is affected by steel wire located in a tire, moreover it was noted that used tires are characterized by higher magnetic field variance than new ones. Areas in a car were also isolated, characterised by different intensity of low frequency magnetic field change.

In the cited articles (GAJŠEK et al. 2010) the focus was mainly on determining magnetic field distribution in different vehicles as well as on the influence of this magnetic field on human health. It was concluded that car tires create magnetic field. Statistical parameters e.g. maximum value, minimum value and peak to peak value were used to describe changes in magnetic field (MILHAM et al. 1999). It was also determined by what sensors a wheel magnetic field may be measured. Nevertheless none of the discussed works concerned research of magnetic field changes caused by puncture e.g. with a ferromagnetic penetrator.

Knowing changes of the magnetic field caused by puncture one may create opportunity to create a system which will warn the driver about possible puncture of a tire on the basis of changes in the magnetic field as a result of tire penetration.

At the moment 3 patent solutions concerning registration of tire magnetic field changes are known. Two US patents 6404182 B1 (*Method for detecting the magnetic field of a tire*) and US 6246226 B1 (*Method and apparatus for detecting tire revolution using magnetic field*) describe a way of measuring rotational speed and distance travelled by previously magnetized wheel (KAWASE, TAZAKI 2001, KAWASE et al. 2001). Polish patent 401304 (22)2012 10 22 (*The method of measuring wheel speed of a road vehicle and the system for measuring wheel speed of a road vehicle*) uses changes in wheel's natural magnetic field to register changes in angular speed of wheel. In the latter solution changes in the magnetic field are registered by a sensor mounted in a car. Other solutions require mounting additional elements which may influence the obtained results (BROL et al. 2014). Because of variety of technical solutions for measuring changes in magnetic field generated by a spinning wheel it was decided to build original measuring stand, which assures measurement of changes in magnetic field of a tire caused by puncture with ferromagnetic penetrator in a repeatable and controlled way.

The main assumption was to arrange magnetic flux density measurements in function of rotation angle which was not done by the predecessors because they applying magnetic flux density measurements in time domain. A measurement in function of wheel rotation angle enables a comparison of a state of a magnetic field both before and after puncture, if the examined wheel does not change its angular location to the spindle of the device during puncture.

## Methodology of data gathering and analysis of the results

The research was carried out by using an original measuring device designed by Szegda and Brol. Devices kinematic diagram was shown in Figure 1a (BROL, SZEGDA 2017, SZEGDA, BROL 2017) and variability ranges of its parameters were shown in Table 1.

Table 1

Physical quantity and value of measurement device			
Physical quantity	Value	Physical quantity	Value
Mass	40 kg	Measuring projections of <b>B</b> vector	3, ( $B_x, B_y, B_z$ )
Height	1022 mm	Sample frequency	75 Hz
Width	867 mm	Spindle speed	0.052–0.52 rad/s
Rims diameter	from 12" for 21"	Angular resolution	0.0015 rad
Kind of rims	Steel/light alloy	Type of <b>B</b> sensor	HMC5883L

A characteristic feature of the device is the fact that the magnetic flux density (**B**) sensor is located in a measuring arm, which enables carrying out research in different distances and orientation to the wheel rotation axis. Measurement and electric engines steering is done by the two separate microcontrollers (Fig. 1b) intentionally located in different places to eliminate their mutual influence and minimize mutual interference.

Moreover the device enables examination of either a wheel or a tire due to the fact that two different fixtures were designed.

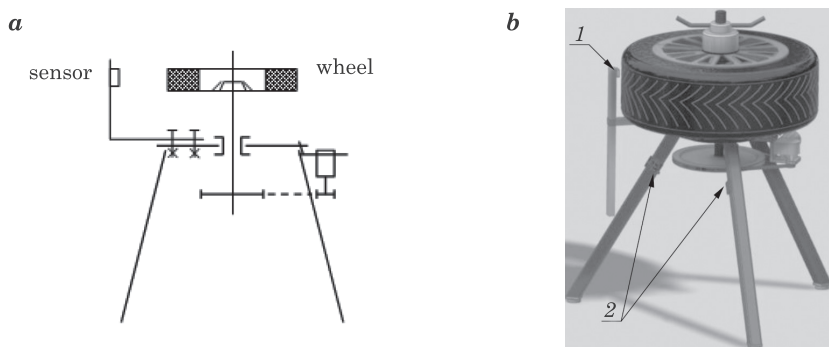


Fig. 1. Kinematic diagram of the measuring device (a) and the measuring device (b), where:  
 1 – measuring sensor, 2 – microcontrollers, respectively measuring and steering  
 Source: a – BROL, SZEGDA (2017), b – SZEGDA, BROL (2017).



The effect of the measurement is so called magnetic profile, consisting of organized values of one of magnetic flux density vector  $\mathbf{B}$  constituents, as shown in Figure 2. It may be measured at sensor mounting point in three measuring directions  $B_x, B_y, B_z$ .

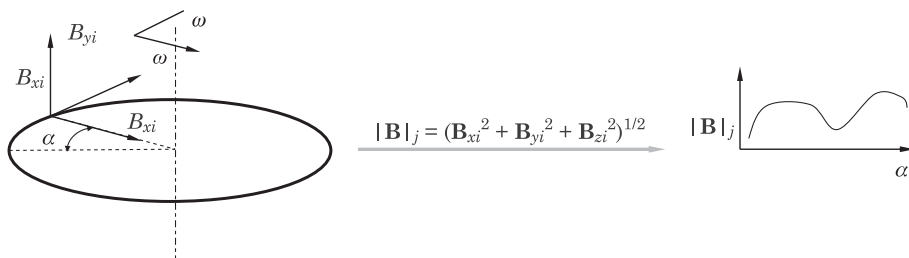


Fig. 2. Sensor orientation and magnetic profile creation diagram

Resultant profiles  $|\mathbf{B}|$  were subject to further analysis. The  $|\mathbf{B}|$  was chosen in this case because it counts changes at three measuring directions.

An object of the research was a radial tire (175/70 R14). The measuring sensor was located 55 mm over the tread of the tire and 765.5 mm from the ground.

At the beginning a measurement was done which was considered to be referential. An opening was made in tread with a 2 mm diameter drill. Next a ferromagnetic penetrator (a screw used for wood screwing) was screwed into an opening. After the penetrator was inside the opening, another measurement was made. The 2 mm diameter drill was chosen because in this case drilling did not tear steel belt wires and thus it did not alter magnetic signature of the wheel. Only screw penetration altered magnetic field of a tire (and of course the wheel). During the experiments wood screws of different, origin, diameters, and lengths served as penetrators as shown in Table 2. The different origin of wood screws were chosen to check if it may influence on results alignment. Moreover the puncture may be caused by different randomly distributed objects laying on the road.

Table 2

Diameter and length of the ferromagnetic penetrators used in research

Penetrator's number	Diameter [mm]	Length [mm]
1	2.5	10
2	2.8	20
3	3.7	25
4	4.7	27

Magnetic profiles were analyzed before and after penetration as well as their parameters and differential profile (a series of results of algebraic subtractions of magnetic flux density before and after puncture for the same angular position along profile) as well as parameters of differential profile. This procedure was repeated four times for every penetrator. Thus obtained profiles were analysed by using statistical parameters and adopted from surface roughness analysis, described by formulas (1–6), presented in the Table 3.

Table 3

Parameters of magnetic profiles

Parameter name	Unit	Formula	Formula number
Minimum value	$\cdot 10^{-7}$ T	$M_{\min} = \min. (B_i)$	(1)
Maximum value	$\cdot 10^{-7}$ T	$M_{\max} = \max. (B_i)$	(2)
Peak to peak value	$\cdot 10^{-7}$ T	$M_m = M_{\max} - M_{\min}$	(3)
Average value of ordinary of profile	$\cdot 10^{-7}$ T	$M_5 = \frac{\sum_{i=1}^N B_i^3}{N}$	(4)
Skewness of distribution of ordinates	$(10^{-7} \text{ T})^3$	$M_5 = \frac{\sum_{i=1}^N B_i^3}{N}$	(5)
Kurtosis of distribution of ordinates	$(10^{-7} \text{ T})^4$	$M_k = \frac{\sum_{i=1}^N B_i^4}{N}$	(6)

$B_i$  – measured magnetic flux density value described by  $i$  index,  $i$  – measurement number around the perimeter from 1 to  $N$ .

## Results

### Analysis of profiles before and after puncture

At the first part of examinations the magnetic profiles of  $|\mathbf{B}|$  were compared before and after puncture. In all cases the differences are barely visible. The reason for that is that the penetrator caused magnetic flux density changes of several dozen  $10^{-7}$  T while  $|\mathbf{B}|$  values in profiles changed values in a range of more than a thousand  $10^{-7}$  T. The penetrator introduced changes 100 times smaller than range of profile variability. Obviously magnetic flux density changes depend on the distance between sensor and tread but in this case (55 mm from a tread) change in values for this examined wheel caused by penetrators were of several dozens  $10^{-7}$  T. It is especially visible in Figure 3 after puncture it with the penetrator 2 (Fig. 3b) and biggest ferromagnetic penetrator (Fig. 3c).

In case of  $M_{\min}$ ,  $M_{\max}$  and  $M_m$  parameters (Tab. 3) which represents the smallest and the highest value of  $|\mathbf{B}|$  in profile, the values change in this case is caused rather by measurement noise than by penetrator itself because

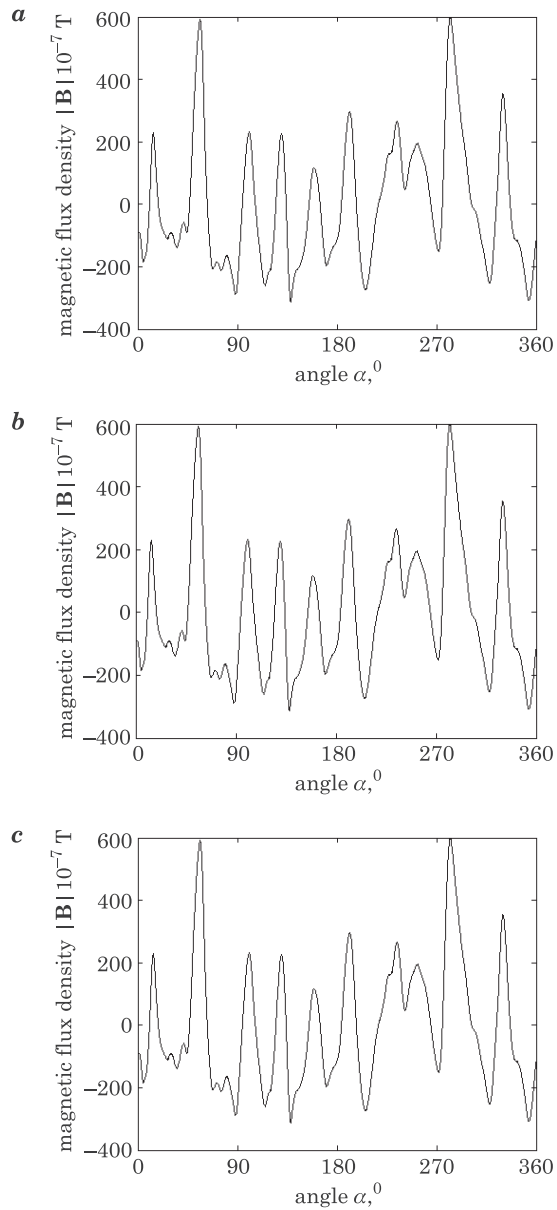


Fig. 3. Magnetic profiles of  $|\mathbf{B}|$ : referential (a), and after penetration with penetrator 2 (b), penetrator 4 (c)

Table 3

Average values of parameters describing changes of magnetic profiles before and after puncture made by ferromagnetic penetrator

Penetrator number	Reference		After puncture	
	$M_{\min}$	$M_{\max}$	$M_{\min}$	$M_{\max}$
1	-312.48	606.21	-312.95	606.53
2	-313.59	597.00	-313.24	596.40
3	-314.34	598.90	-313.80	598.62
4	-313.50	597.84	-313.59	597.92
	$M_m$	$M_b$	$M_m$	$M_b$
1	918.69	166.38	919.48	166.29
2	910.60	165.48	909.64	165.61
3	913.24	165.76	912.42	165.68
4	911.34	165.45	911.52	165.55
	$M_s$	$M_k$	$M_s$	$M_k$
1	0.79	3.14	0.79	3.14
2	0.82	3.21	0.81	3.21
3	0.82	3.22	0.82	3.22
4	0.82	3.22	0.82	3.22

the puncture place is not in the same angular position with max and min value of profile. Only if such alignment will happen the  $M_{\min}$ ,  $M_{\max}$  and  $M_m$  would be sensitive to tire damage.

The  $M_b$  parameter represents the mean value and therefore should be not sensitive to noise with median equal to zero. Since measurement noise may be assumed to be constant and sample count is sufficient (2048) than any change in  $M_b$  value should be caused by profile shape change – the effect of penetration. The difference in this investigations are about 0.1 to 0.2 · 10<sup>-7</sup> T, which suggest that this value, because of its averaging property, “reacts” with very small increase on puncture. The same can be told about  $M_k$  and  $M_s$  parameters.

### Analysis of differential profiles

At the next stage of investigations differential profiles (Fig. 4) of value |B| were analyzed.

The differential signal shown in Figure 4a differs from others. The signal course and distribution is similar to that of magnetic sensor when no magnetic field of tire were present during measurement. Therefore, it can be concluded that penetration with a 2.5 mm screw does not change the image of the measured magnetic field. This can be explained by the fact that, as a result of drilling and subsequent screwing, the steel belt was not damaged (see Fig. 5).

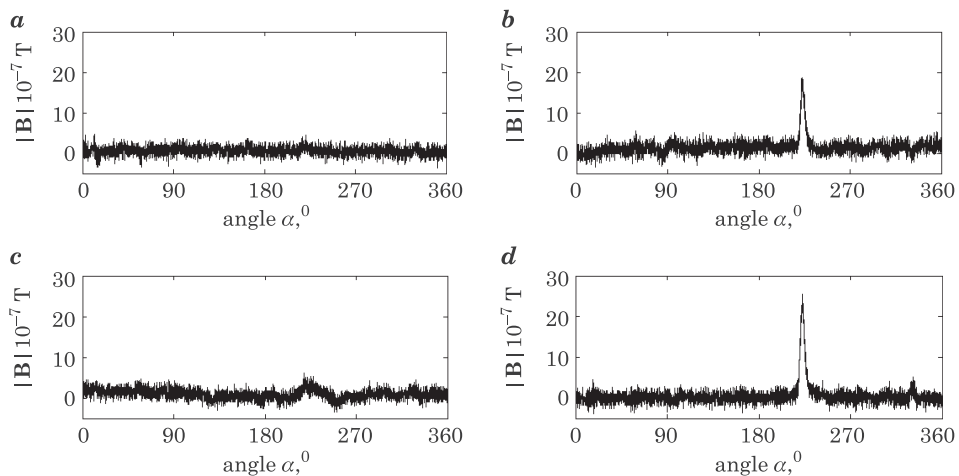


Fig. 4. Differential profiles after puncture for used penetrators

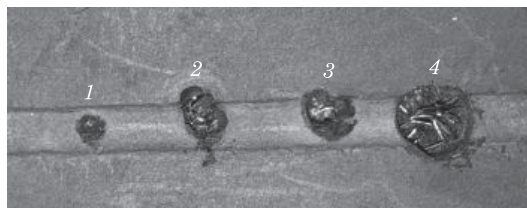


Fig. 5. Holes after penetration. Good visible damage to the belt, especially in the second and fourth hole

A drill with a diameter of 2 mm and later a 2.5 mm screw penetrated the tire in such a way that it did not damage the belt wires. The belt is made of two layers of wire one over the other. The wires in each layer are guided parallel to each other and at an angle to the longitudinal axis of the tread. The lower layer has already routed wires from another angle.

From this it follows that if the penetrator has a sufficiently small diameter it does not damage the belt and thus does not change the magnetic field of the tire in a detectable manner with the measuring instrument used in these tests. This can be due to a circumferential resolution (0.46 mm) for this measurement device settings and for this free wheel radius. In addition, the distance between the sensor and the tread (55 mm) may be too large for this specific penetrator (3.7 mm in diameter). Farther investigation will be performed in the future to settle this dilemma.

In the signal before and after the penetration, a clear “peak” was observed at the penetration site of the tire in three of four cases (Fig. 4b–d).

The largest “peak” was observed after using Ø4.7 mm diameter penetrator, which was greater than the peak after penetration of 2.8 mm by  $6.8 \cdot 10^{-7}$  T. Interestingly, the 3.7 mm penetrator generated the smallest “peak” in these tests. It is assumed that this may be due to other magnetic properties of the material used for its production than for the other penetrators. Parameter values describing differential profiles are summarized in Table 4.

Table 4

Selected values of parameters of differential magnetic profile

Differential profile parameters	Number of penetrator			
	1	2	3	4
$M_{\min}$	-3.61	-3.56	-3.58	-3.87
$M_{\max}$	4.74	18.55	6.23	25.43
$M_m$	0.55	1.33	0.94	0.40
$M_b$	1.09	1.94	1.26	2.23
$M_s$	-0.02	3.03	0.06	5.49
$M_k$	3.14	23.91	3.16	47.74

It can be noted that all the parameters applied on differential profiles (beside  $M_{\min}$ ) change their values due to the tread break. The smallest changes were observed for the impact of penetration with a penetrator of 3.7 mm in diameter but further mean values were higher than for that penetrator of 2.5 mm diameter.

The greatest increase in values was observed for the  $M_k$  parameter (Fig. 6). The  $M_k$  value describes the statistical moment of the fourth order of distribution of the ordinates of the profile and is therefore sensitive (as  $M_s$ ) to the local peaks. The mean value of  $M_s$  as a result of the puncture changed from a negative near zero (actually oscillating around zero) to positive.

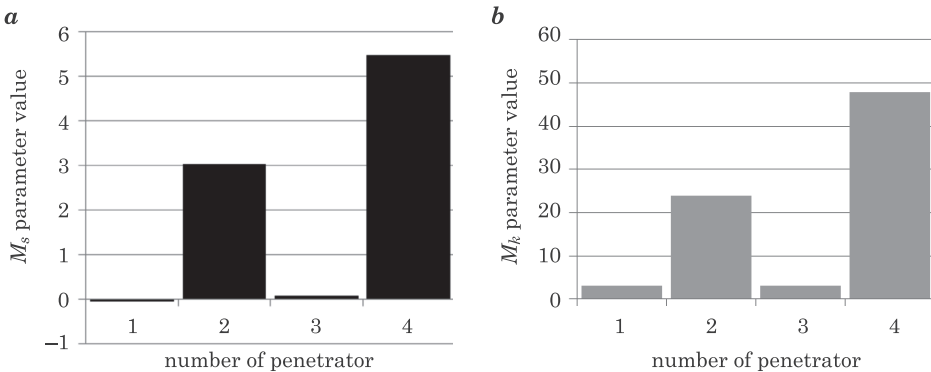


Fig. 6. Parameter values  $M_s$  and  $M_k$  for different penetrators calculated on signals which represents difference of magnetic profiles before (a) and after (b) puncture

The authors state that the most useful parameter in this application is the  $M_b$  parameter (Fig. 7). As the average ordinary profiles, it is insensitive to local peaks and disturbances, but its value has increased by at least as much as 15% (for a 3.7 mm penetrator and for other much more) after penetration. This implies that the “punctured peak” has the shape of an inverted or relatively wide funnel, and this type of profile shape has a significant effect on the value of the  $M_b$  parameter.

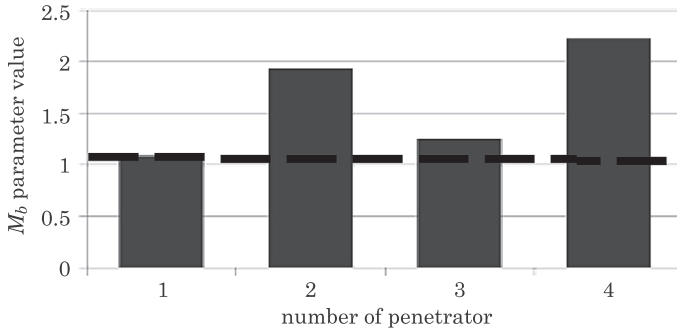


Fig. 7.  $M_b$  parameter value for differential magnetic profiles before and after puncture for different penetrators

## Summary

Puncture detection based on quality analysis of profiles before and after penetration with a ferromagnetic penetrates is difficult, because the changes in the magnetic field caused by the penetration itself are small. The changes in the magnetic field caused by the penetration itself are two magnitudes smaller than the changes in the magnetic flux density variability prior to the penetration.

The quantitative analysis using parameters defined by the dependencies (1–6) also does not provide any information about the penetration.

The magnetic profiles before and after puncture are different. It can be clearly see a characteristic peak at the puncture angle. The peak height seems to be correlated with the distance between the sensor and the tread and the size of the penetrator.

The material of the penetrator plays a significant role. It is especially visible while using a penetrator with a 3.7 mm diameter. The peak height also could give an insight to the damage of the belt. The differential profile (of the magnetic profiles before and after the puncture) allow to collect the data about the perforated tire. In order to detect differences caused by puncture it is recommended use the values of  $M_b$ ,  $M_s$  and  $M_k$ . It is necessary to keep in mind that  $M_s$  and  $M_k$  are very susceptible towards noise, thus it might be problematic to apply them on magnetic profiles obtained from road studies.

## References

- BROL S. 2013. *Analiza możliwości wykorzystania bezpośredniego pomiaru przyspieszenia do wyznaczania właściwości trakcyjnych samochodu osobowego*. Oficyna Wydawnicza Politechniki Opolskiej, Opole.
- BROL S., PRAŻNOWSKI K, AUGUSTYNOWICZ A. 2014. *Sposób pomiaru prędkości obrotowej koła ogumionego pojazdu drogowego i układ do pomiaru prędkości obrotowej koła ogumionego pojazdu drogowego*. MKP, Politechnika Opolska. Patent, Polska, nr PL 223767, 2014.
- BROL S., SZEGDA A. 2017. *Prototypowe urządzenie do pomiaru zmian indukcji generowanej przez obracające się koło samochodowe*. *Pomiary Automatyka Robotyka*, 1: 51–56.
- BROL S., SZEGDA A. 2017. *Direct measurement of magnetic flux density of car's wheels*. *Proceedings of the Institute of Vehicles*, 2(111): 37–44.
- CHMIELEWSKI A., RADKOWSKI S., SZULIM P. 2013. *Badania Czujnika Flux-Gate*. *Zeszyty Naukowe Instytutu Pojazdów*, 5(96).
- GAJSEK P., RAVAZZANI P., GRELLIER J., SAMARAS T., BAKOS J., THURÓCZY G. 2010. *Review of Studies Concerning Electromagnetic Field (EMF) Exposure Assessment in Europe: Low Frequency Fields (50 Hz–100 kHz)*. *Radiation Protection Dosimetry*, 141(3): 255–268.
- GONTARZ G., RADKOWSKI S. 2011. *Magnetic Methods in Diagnosis of Machines and Infrastructural Objects – A Survey*. *Diagnostyka – Diagnostics and Structural Health Monitoring*, 1(57).
- JENS B. 2002. *EFM Measurements of Cars and Trucks*. <http://www.eiwellspring.org/ehs/emfmeasurementsofcarsandtrucks.pdf> (access 3.07.2018).
- KAWASE M., TAZAKI S. 2001. *Method for detecting the magnetic field of a tire*. US 6404182 B1.
- KAWASE M., TAZAKI S., KANEKO H., SATO H., URAYAMA N. 2001. *Method and apparatus for detecting tire revolution using magnetic field*. US 6246226 B1.
- MILHAM S., HATFIELD J. B., TELL R. 1999. *Magnetic Fields From Steel-Belted Radial Tires: Implications for Epidemiologic Studies*, *Bioelectromagnetics*, 20: 440–445.
- STANKOWSKI S., KESSI A., BÉCHEIRAZ O., MEIER-ENGEL K., MEIER M. 2003. *Low frequency magnetic fields in cars, induced by tire magnetisation*. Work was supported by the Swiss Federal Office of Public Health, Berne, Switzerland, grant numbers: 02.000277/02.001005/03.0005427/03.000542.
- SZEGDA A., BROL S. 2017. *Measurement device of magnetic flux density of tire*. *Proceedings of the Institute of Vehicles*, 2(111): 121–128.





## EFFECT OF TEMPERATURE, CONCENTRATION OF ALCOHOLS AND TIME ON BAKER'S YEAST PERMEABILIZATION PROCESS

*Ilona Trawczyńska, Justyna Milek, Sylwia Kwiatkowska-Marks*

Department of Chemical and Biochemical Engineering  
Jan and Jędrzej Śniadecki University of Technology and Life Sciences in Bydgoszcz, Poland

Received 16 February 2018, accepted 2 July 2018, available online 8 October 2018.

**Key words:** permeabilization, baker's yeast, biocatalyst, response surface methodology.

### Abstract

Baker's yeast beyond the traditional use in the food industry may be used to carry out biotransformations. The effectiveness of yeast as biocatalysts is based on the presence of large amounts of intracellular enzymes, whose efficiency can be repeatedly increased by permeabilization. It is the process of increasing the permeability of cell walls and membranes in order to facilitate reagents access to the intracellular enzyme. Alcohols permeabilization process allows for approx. 50-fold increase in catalase activity of baker's yeast. In this paper, the influence of physical and chemical parameters on the effectiveness of permeabilization of baker's yeast cells using alcohols was analyzed. Research has shown that with increasing temperature of permeabilization process better results are achieved using a lower alcohol concentration. Based on presented response surface graphs, we can also indicate a negligible impact of duration time on the process efficiency.

### Abbreviations

$T$  – temperature

$S$  – concentration

$t$  – time

RSM – response surface methodology

## Introduction

As the name suggests, baker's yeast are microorganisms used in food industry, particularly in bakery products. For thousands of years they have served as an ingredient for dough leavening. Carbon dioxide evolved due to their fermentation ability causes the dough to leaven, transforming it into bakery products with a spongy and porous structure. Apart from the fermentation processes, baker's yeast is used in intensively developing processes of food products enrichment, i.e. fortification (GONCERZEWICZ, MISIEWICZ 2011) as well as in microencapsulation of e.g. food aromas (WOJTYŚ, JANKOWSKI 2004) and vitamins (CZERNIAK, JANKOWSKI 2013). Baker's yeast, due to its high content of various intracellular enzymes, has also found an application as catalyst in bioprocesses. They are a rich source of catalase – one of the most industrially significant enzyme in view of the ability to degrade  $H_2O_2$  into water and oxygen.

Many scientists have proven that the use of biocatalysts in the form of whole cells of microorganisms is often more effective than the use of purified enzymes (SEKHAR et al. 1999, VENKATESHWARAN et al. 1999, XU et al. 2016). However, low permeability of cell wall and membrane contributes to the slow rate of reactions catalyzed by whole cells enzymes. Such difficulties can be overcome by the application of permeabilization technique which is to improve the permeability of cell wall and membrane of microorganisms for facilitating the diffusion of reaction reagents, while also maintaining the cell's properties, including enzymatic activity and structure.

The most common technique of increasing permeability of cell membranes is chemical permeabilization with the use of detergents (CHOW, PALECEK 2004, GOUGH et al. 2001, KIPPERT 1995, PATIL et al. 2017, PRESECKI, VASIĆ-RACKI 2005) and organic solvents (KONDO et al. 2000, KUMARI et al. 2011, PANESAR et al. 2007). The literature data show that the choice of a chemical agent is dependent on the type of a permeabilized microorganism (CHOW, PALECEK 2004, GALABOVA et al. 1996). Additionally, applied agent should not affect the activity of intracellular enzymes. Therefore, in order to determine the optimal conditions of the process for selected microorganisms, it is necessary to analyze the influence of numerous various substances on their permeability, thus determining the most effective one. Chemical permeabilization of yeast carried out with the use of detergents causes considerable changes in the cell membrane structure, in comparison to organic solvents. This, in consequence, leads to cellular leakage or even to its destruction (ALAMAE, JARVISTE 1995). For this reason if the second reaction with the use of the same biocatalysts is necessary, it is not advised to obtain them by the application of permeabilization method with the use of detergents, but to select the most effective permeabilizing agent from among alcohols.

The increase in permeability of cell wall and membrane of microorganisms is determined not only by the type of permeabilizing agent but also the operating conditions. This study aims to determine the effect of temperature ( $T$ ), concentration of the chemical substance ( $S$ ) and treatment time ( $t$ ) of the permeabilization process on its effectiveness. The intent is to determine the influence of mutual interactions of analyzed parameters on the effectiveness of the process. For this purpose the response surface methodology has been applied in the study. The effectiveness of the process has been represented by measuring intracellular catalase activity.

## **Materials and methods**

### **Biological material and chemical reagents**

The producer of baker's yeast (*Saccharomyces cerevisiae*) is Lasaffre bio-corporation S.A. from Wolczyn, Poland. A fresh block of moist yeast was stored in accordance with the producer's recommendations, at a temperature below 10°C. For the whole duration of the study the yeast maintained the moisture content of 68.5%. Organic solvents have been used, i.e. ethanol (ethyl alcohol), 1-propanol and 2-propanol. Catalase activity was assayed with the use of hydrogen peroxide 30%, phosphate buffer pH 7 and nitrogen gas from EuroGaz Gdynia. All the chemical reagents mentioned above (except the nitrogen) were pure for the analysis, obtained from POCh S.A. Gliwice.

### **Permeabilization process**

1 g of baker's yeast and 20 g of a permeabilizing agent were placed into a 50 cm<sup>3</sup> beaker. The concentration of alcohol was according to the selected plan of experiments. With the use of a mechanical stirrer the biological material was distributed appropriately. The suspension was vigorously stirred using a water-bath with a shaking mechanism. The device enabled to conduct the permeabilization process at an appropriate temperature (according to the plan of experiments). After an appropriate amount of time, according to the plan, a sample of yeast cells was taken and their intracellular catalase activity was assayed with a method described below.

## Catalase activity assay

The catalase activity was determined using an oxygen method. For this purpose the increase in dissolved oxygen resulting from the enzymatic decomposition of hydrogen peroxide was measured. A detailed description of the process was presented in previous publications (TRAWCZYŃSKA, WÓJCIK 2014, TRAWCZYŃSKA, WÓJCIK 2015).

## Response surface methodology

Study on the effects of physico-chemical parameters on the effectiveness of permeabilization process of baker's yeast cells was conducted in accordance with the principle of optimization of chemical processes using response surface methodology. This method is a set of statistical and mathematical techniques used in developing, improving and optimizing processes. In the RSM algorithm

Table 1

Central composite design matrix

No	Temperature	Concentration	Time	Enzyme activity [ $\text{U}\cdot\text{g}^{-1}$ ]		
				ethanol	1-propanol	2-propanol
1	-1	-1	-1	190	140	230
2	-1	1	-1	2,540	3,410	4,840
3	-1	-1	1	260	235	1,990
4	-1	1	1	3,085	2,560	5,050
5	1	-1	-1	620	340	2,690
6	1	1	-1	2,040	2,580	4,990
7	1	-1	1	2,120	1,620	3,620
8	1	1	1	1,780	1,935	3,600
9	1.682	0	0	140	1,370	2,570
10	-1.682	0	0	210	1,135	360
11	0	1.682	0	1,005	2,210	4,980
12	0	-1.682	0	300	140	120
13	0	0	1.682	4,340	3,590	4,760
14	0	0	-1.682	1,690	2,570	3,090
15	0	0	0	4,390	4,100	5,900
16	0	0	0	5,070	4,220	5,750
17	0	0	0	5,150	4,070	5,880
18	0	0	0	5,050	3,970	5,780
19	0	0	0	4,760	4,170	5,800
20	0	0	0	5,190	4,145	5,765

of action, variables that significantly affect the process are being tested simultaneously in the minimal number of runs. Therefore, this method is less expensive and less time-consuming compared to classical methods. In RSM, geometrical images of a response function are used. These are plots which represent a set of experimental results according to the plan of experiments. The research program was designed in such manner, that it was possible to obtain the necessary information performing the fewest number of analysis possible. Therefore, the research was conducted according to the points of the compositional design, plan which in the form of coded variables is given in Table 1. The number of necessary experiments to conduct was 20 for each of the permeabilization processes, i.e. with the use of ethanol, 1-propanol, 2-propanol.

## Results and discussion

### Measuring ranges

Table 2 shows measuring ranges for agents affecting the permeabilization process of baker's yeast cells with selected alcohols, determined on the basis of preliminary investigations.

Table 2

Measurement ranges	Measurement ranges								
	Ethanol			1-Propanol			2-Propanol		
	<i>T</i> [°C]	<i>S</i> [%]	<i>t</i> [min.]	<i>T</i> [°C]	<i>S</i> [%]	<i>t</i> [min.]	<i>T</i> [°C]	<i>S</i> [%]	<i>t</i> [min.]
-1.682	6.6	24.8	7	1.5	3.2	7	6.6	6.4	7
-1	10	35	20	5	10	20	10	20	20
0	15	50	40	10	20	40	15	40	40
1	20	65	60	15	30	60	20	60	60
1.682	23.4	75.2	73	18.5	36.8	73	23.4	73.6	73

### Response surface plots

In order to perform an accurate analysis of the process behavior within the limits of the experiment, response surface plots were created. They were based upon experiments conducted in the points of compositional plans (TRAWCZYŃSKA, WÓJCIK 2014, TRAWCZYŃSKA, WÓJCIK 2015). Plots present an effect of two process variables on activity of catalase, assuming that the value of the third variable is constant.

Response surface plot (Fig. 1a), depicting catalase activity (i.e., effectiveness of the process) as a function of temperature and alcohol concentration, indicates a gradual increase of activity with the increase of analyzed parameters, up to the alcohol concentration of approx. 50% and the temperature of approx. 15°C. With a further increase of both variables a decrease of enzyme activity can

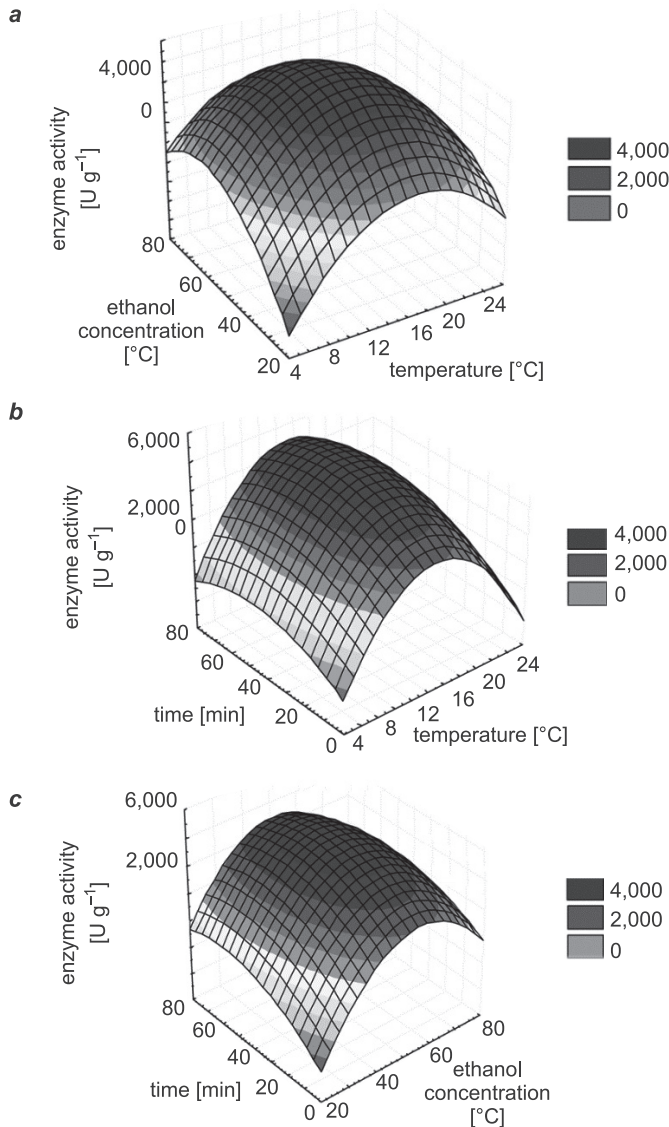


Fig. 1. Response surface plots for permeabilization of baker's yeast cells using ethanol; the effect of: *a* – temperature and ethanol concentration, *b* – temperature and permeabilization time, *c* – ethanol concentration and permeabilization time

be noticed. This can be explained by that fact that alcohol concentration and temperature of the process increase up to certain values, for which it is possible to observe the maximal catalase activity. Once the values are exceeded, a correlation can be observed, indicating that the higher the solvent concentration and temperature are, the lower the enzyme activity is. This correlation can be caused by deactivation of the enzyme in higher concentrations of alcohol or higher temperatures. Low effectiveness of permeabilization at low concentrations can be explained by an insufficient amount of solvent.

According to the data presented in Figure 1*b*, the effectiveness of permeabilization of baker's yeast increase with the increase of temperature at which the process has been performed. Once the temperature of approx. 15°C is exceeded the response plot breaks and falls, which can be caused by the thermal deactivation of enzyme. Surfaces in Figure 1*b* and 1*c* depict the influence of the treatment time of the process on its effectiveness. Optimum (4,900–5,100 U·g<sup>-1</sup>) can be observed within a wide range of time. Consequently, this leads to conclusion that the parameter has a slight effect on the process.

The plot presenting the dependence of catalase activity on the concentration of 1-propanol and temperature (Fig. 2*a*) indicates high enzyme activity (4,000 U·g<sup>-1</sup>) within temperature and alcohol concentration ranges of 8–12°C and 15–25% respectively. Below and above those ranges a significant decrease of effectiveness of permeabilization can be noticed. Plot presented in Figure 2*b* is a graphical representation of the dependence of catalase activity on temperature and treatment time of the process at a constant concentration of alcohol solution. Dominant influence of the first of analyzed variables on the shape of the plot is noticeable. Convex response surface possesses a breaking point (2,980–3,100 U·g<sup>-1</sup>) within temperature range of 8–12°C. Figure 2*c* depicting catalase activity in the concentration function of 1-propanol and treatment time of the process is determined mainly by the first parameter. Enzyme activity increases in the concentration ranging from 0 to 15%, and the plot takes the form of a plane with a certain inclination angle. In the areas of higher concentrations a smooth curvature of the plot can be noticed, where the activity maintains the level of 4,000 U·g<sup>-1</sup>. The response plots in Figure 2*b* and 2*c*, similar to the permeabilization with the use of ethanol, present evident optimum within a wide range of time.

Figure 3 depicts 3D response surface plots of catalytic activity depending on temperature, concentration of 2-propanol and treatment time of the process. A parabolic relationship between analyzed parameters of the process is indicated, similar to the permeabilization with the use of ethanol and 1-propanol. According to the data presented in Figure 3*a*, employing low concentrations of alcohol (i.e. below 30%) at low temperatures does not lead to a significant increase of catalytic activity. Similar to the use of high concentrations of alcohol at high temperatures of the process. High catalase activities (approx. 5,800 U·g<sup>-1</sup>)

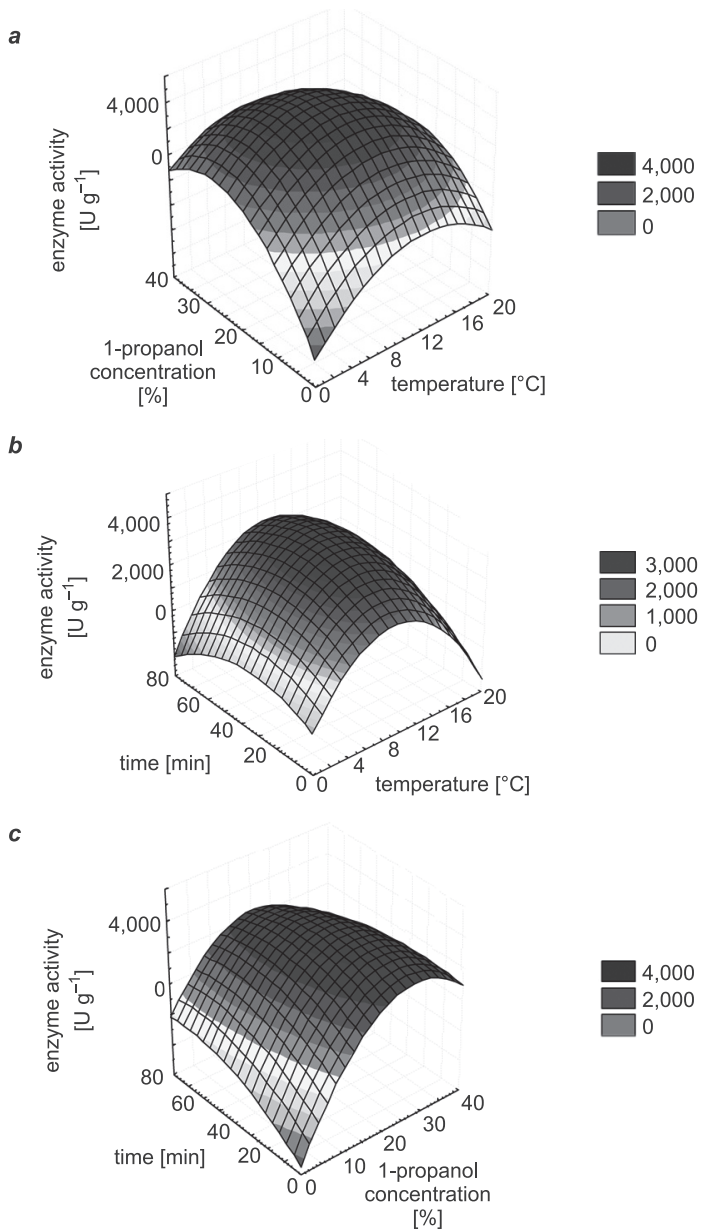


Fig. 2. Response surface plots for permeabilization of baker's yeast cells using 1-propanol; the effect of: *a* – temperature and 1-propanol concentration, *b* – temperature and permeabilization time, *c* – 1-propanol concentration and permeabilization time



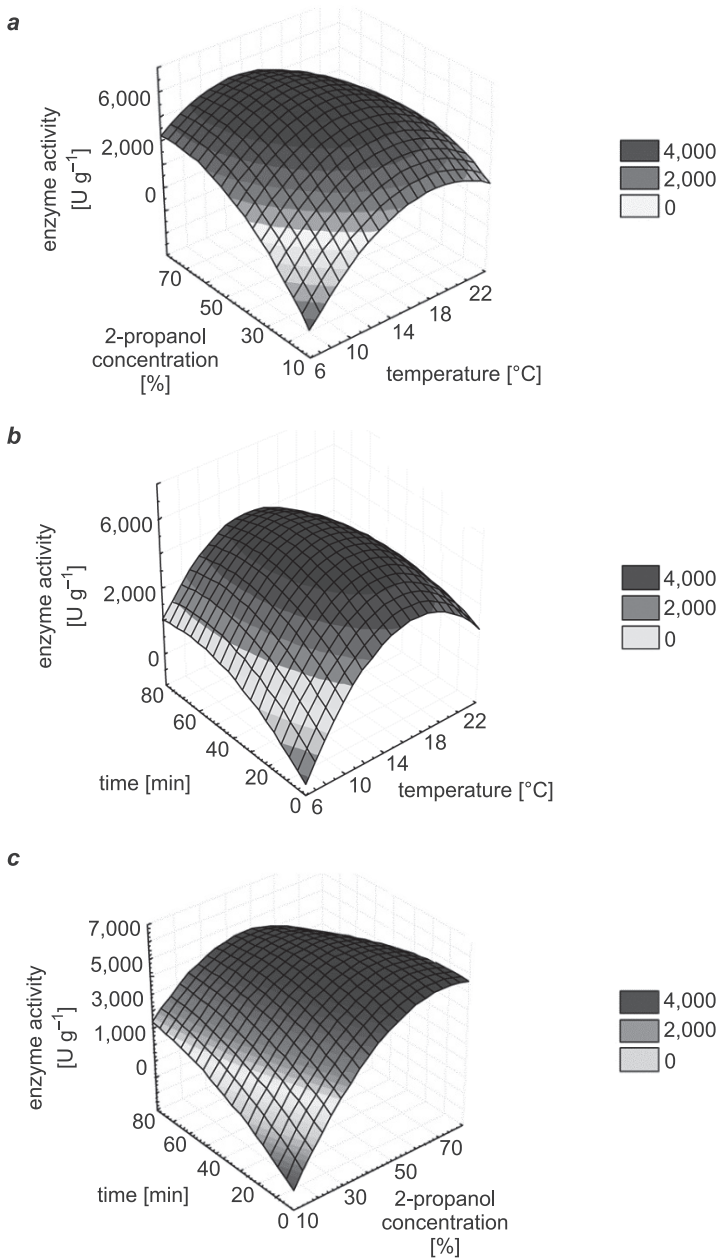


Fig. 3. Response surface plots for permeabilization of baker's yeast cells using 2-propanol; the effect of: *a* – temperature and 2-propanol concentration, *b* – temperature and permeabilization time, *c* – 2-propanol concentration and permeabilization time

maintain their level within the temperature range of 10–20°C and 2-propanol concentration range of 40–60%.

Performed tests indicate temperature and alcohol concentration as significant factors affecting the process of permeabilization of baker's yeast. At the same time the tests demonstrate little relevance on the process when it comes to the treatment time. Similar results have been achieved by PANESAR et al. (2007). Those experiments have been conducted with the use of alcohols as a permeabilizing agent, however, in the permeabilization process of yeast cells *Kluyveromyces*, not baker's yeast. Moreover, the effectiveness of the process was based upon measurements of  $\beta$ -galactosidase intracellular activity. By comparing the planes for the permeabilization of baker's yeast with the use of specific alcohols, conclusions can be drawn that 2-propanol enables to achieve the highest enzymatic activity. Nevertheless, yeast cells of similar effectiveness can be achieved employing ethanol in permeabilization process. The advantage of ethanol, however, is the fact that it is safer alcohol, that can be utilized in food industry without any significant restrictions. Thereby, yeast cells permeabilized with ethanol are considered significantly attractive biocatalysts.

### Mathematical models

Mathematical models determining dependence of catalase activity ( $A$ ) on the parameters of permeabilization process form a quadratic equation in three variables (Tab. 3). They can be used in permeabilization process simulation within the tested parameters: temperature ( $T$ ), concentration of alcohol ( $S$ ) and time ( $t$ ).

Table 3

Mathematical models

Ethanol	$A_E = 4,919 + 545 \cdot S_E + 464 \cdot t_E - 1,574 \cdot T_E^2 - 1,405 \cdot S_E^2 - 570 \cdot t_E^2 - 512 \cdot T_E \cdot S_E$
1-Propanol	$A_{1P} = 4,116 + 851 \cdot S_{1P} - 1,032 \cdot T_{1P}^2 - 1,059 \cdot S_{1P}^2 - 386 \cdot t_{1P}^2 - 378 \cdot T_{1P} \cdot S_{1P} - 358 \cdot S_{1P} \cdot t_{1P}$
2-Propanol	$A_{2P} = 5,784 + 477 \cdot T_{2P} + 1,327 \cdot S_{2P} - 1,343 \cdot T_{2P}^2 - 960 \cdot S_{2P}^2 - 473 \cdot t_{2P}^2 - 675 \cdot T_{2P} \cdot S_{2P} - 484 \cdot S_{2P} \cdot t_{2P}$

The analysis of variance (ANOVA) results shows that the regressions are highly significant and present good determination coefficients ( $R^2_E = 0.974$ ,  $R^2_{1P} = 0.981$ ,  $R^2_{2P} = 0.977$ ). The closer the  $R^2$  is to 1, the stronger the model is and the better it predicts the response.

## Conclusions

Based upon the research, conclusion can be drawn, that alcohol of lower concentration provides better results, along with the increase of temperature in permeabilization process of baker's yeast cells. Applying solvents of too high concentrations contribute to the decrease of permeabilization effectiveness. At high temperatures of approx. 20°C, better results can be achieved by applying lower concentrations of alcohol, along with the increased duration of cells shaking. Treatment time of the process proved to be a parameter bearing little influence on the effectiveness of the process.

### Acknowledgements

The authors are thankful to Professor Marek Wójcik for providing valuable comments and feedback at various stages of this research.

## References

- ALAMAE T., JARVISTE A. 1995. *Permeabilization of the methylotrophic yeast Pichia pinus for intracellular enzyme analysis: a quantitative study*. Journal of Microbiological Methods, 22(2): 193–205.
- CHOW C.K., PALECEK S.P. 2004. *Enzyme encapsulation in permeabilized Saccharomyces cerevisiae cells*. Biotechnol Progress, 20(2): 449–456.
- CZERNIAK A., JANKOWSKI T. 2013. *Mikrokapsułkowanie  $\alpha$ -tokoferolu wewnątrz komórek drożdży Saccharomyces cerevisiae*. Żywność. Nauka. Technologia. Jakość, 6(91): 151–164.
- GALABOVA D., TULEVA B., SPASOVA D. 1996. *Permeabilization of Yarrowia lipolytica cells by Triton X-100*. Enzyme and Microbial Technology, 18(1): 18–22.
- GONCERZEWICZ A., MISIEWICZ A. 2011. *Wzbogacanie żywności kwasem foliowym – naturalnym metabolitem przemysłowych szczepów drożdży Saccharomyces cerevisiae oraz bakterii fermentacji mlekowej*. Postępy Nauki i Technologii Przemysłu Rolno-Spożywczego, 66(4): 33–52.
- GOUGH S., DESHPANDE M., SCHER M., ROSAZZA J.P.N. 2001. *Permeabilization of Pichia pastoris for glycolate oxidase activity*. Biotechnology Letters, 23(18): 1535–1537.
- KIPPERT F. 1995. *A rapid permeabilization procedure for accurate quantitative determination of beta-galactosidase activity in yeast cells*. FEMS Microbiology Letters, 128(2): 201–206.
- KONDO A., LIU Y., FURUTA M., FUJITA Y., MATSUMOTO T., FUKUDA H. 2000. *Preparation of high activity whole cell biocatalyst by permeabilization of recombinant flocculent yeast with alcohol*. Enzyme and Microbial Technology, 27(10): 806–811.
- KUMARI S., PANESAR P.S., BERA M.B., SINGH B. 2011. *Permeabilization of yeast cells for beta-galactosidase activity using mixture of organic solvents: A response surface methodology approach*. Asian Journal of Biotechnology, 3(4): 406–414.
- PANESAR P.S., PANESAR R., SINGH R.S., BERA M.B. 2007. *Permeabilization of yeast yeasts with organic solvents for  $\beta$ -galactosidase activity*. Research Journal of Microbiology, 2(1): 34–41.
- PATIL M.D., DEV M.J., SHINDE A.S., BHILARE K.D., PATEL G., CHISTI Y., BANERJEE U.C. 2017. *Surfactant-mediated permeabilization of Pseudomonas putida KT2440 and use of the immobilized permeabilized cells in biotransformation*. Process Biochemistry, 63: 113–121.
- PRESECKI A.V., VASIĆ-RACKI D. 2005. *Production of L-malic acid by permeabilized cells of commercial Saccharomyces Sp. Strains*. Biotechnology Letters, 27(23–24): 1835–1839.
- SEKHAR S., BHAT N., BHAT S.G. 1999. *Preparation of detergent permeabilized Bakers' yeast whole cell catalase*. Process Biochemistry, 34(4): 349–354.

- TRAWCZYŃSKA I., WÓJCIK M. 2014. *Application of response surface methodology for optimization of permeabilization process of baker's yeast*. Polish Journal of Chemical Technology, 16(2): 31–35.
- TRAWCZYŃSKA I., WÓJCIK M. 2015 *Optimization of permeabilization process of yeast cells for catalase activity using response surface methodology*. Biotechnology & Biotechnological Equipment, 29: 72–77.
- VENKATESHWARAN G., SOMASHEKAR D., PRAKASH M.H., AGRAWAL R., BASAPPA S.C., JOSEPH R. 1999. *Production and utilization of catalase using Saccharomyces cerevisiae*. Process Biochemistry, 34(2), 187–191.
- WOJTYŚ A., JANKOWSKI T. 2004. *Wpływ temperatury na szybkość przenikania wybranych olejków eterycznych do komórek drożdży piekarskich*. Żywność. Nauka. Technologia. Jakość, 3(40): 77–86.
- XU P., ZHENG G.W., DU P.X., ZONG M.H., LOU W.Y. 2016. *Whole-Cell Biocatalytic Processes with Ionic Liquids*. ACS Sustainable Chemistry & Engineering, 4(2): 371–386.

## EFFECT OF POLYPROPYLENE FIBER ADDITION ON MECHANICAL PROPERTIES OF CONCRETE BASED ON PORTLAND CEMENT

*Marcin Małek<sup>1</sup>, Wojciech Życiński<sup>1</sup>,  
Mateusz Jackowski<sup>1</sup>, Marcin Wachowski<sup>2</sup>*

<sup>1</sup>Department of Building and Military Infrastructure  
Faculty of Civil Engineering and Geodesy

Military University of Technology in Warsaw, Poland

<sup>2</sup>Institute of Mechanical Engineering

Faculty of Mechanical Engineering

Military University of Technology in Warsaw, Poland

Received 12 June 2018, accepted 26 August 2018, available online 8 October 2018.

**Key words:** polypropylene fibers, mechanical properties, concrete, portland cement.

### Abstract

In this work results of poly(propylene) fibers (PP), from recycling process, added into concrete mixture based on portland cement was characterized. The main purpose of this research was to identify direct influence of the fibers addition on the concrete mechanical strength. The recipe of the concrete was prepared using three types of aggregates with different grain size: 0.125–0.250, 0.250–0.500 and 0.500–1.000 mm, deflocculant based on polycarboxylates, water and portland cement (42.5 MPa). To identify structures of the researched samples and fibers light microscopy (LM) observation was performed. Basic properties of concrete mixture were defined by slump cone test and setting time. Mechanical properties such as compressive strength and bending test after 1, 7, 14 and 28 days were characterized. Obtained results were compared with mixtures without fibers modifications. Study was proven that all chosen fibers from recycled origin revealed increased effect on final mechanical properties of concrete and are very perspective for future application in concrete technology.

## Introduction

Negative features of traditional concrete can be eliminated by using dispersed fibers in a concrete mix. Fibers after mixing and binding processes with the concrete form “fiber-concrete composite” with tensile strength and fatigue resistance higher than in traditional concrete (SONG et al. 2005, p. 1546–1550). Concrete provides adequate compressive strength, stiffness of the composite. Fibers provide protection against corrosion, increase tensile strength and reduce shrinkage that causes cracks in the concrete. Both elements complement each other. Due to the application and properties of the composite, fibers were divided into three groups: polymeric (polypropylene), steel and glass and carbon fibers (BANTHIA, GUPTA 2006, p. 1263–1267. KAKOOEI et al. 2012, p. 73–77).

The smallest and lightest are polypropylene fibers, usually added to concrete mix in amount of about  $0.6 \text{ kg/m}^3$ . Due to dispersion of the polymeric fibers, increase of the composite strength in all directions is observed. Addition of the polymeric fibers causes reduction of the contraction of the concrete, especially during its first binding phase (LIMA et al. 2016).

Steel fibers are still the most common used fibers in concrete industry. They cause increase of the tensile and fatigue strength of the hardened composite. They are typically dosed in an amount from  $15 \text{ kg/m}^3$  to  $40 \text{ kg/m}^3$  of a concrete mixture. Steel fibers also limit shrinkage in concrete but only when dosing values is low ( $15 \text{ kg/m}^3$ ). It is also recommended to add polypropylene fibers to steel fibers in the concrete mixture in order to reduce cracks on the concrete surface. Large amount of fibers per cubic meter, in some cases, could replace classical reinforcement almost completely. Steel fibers can also be classified due to their shape and length. Thus, straight fibers, corrugated, curved and in the shape of a letter resembling the letter C or Z are found (CHOUMANIDIS et al. 2016, p. 266–277. SMRKIĆ et al. 2017, p. 893–905).

Macropolymer fibers are in a direct competition with steel fibers. They are characterized primarily by a higher tensile strength, less dosing to the concrete mix and the fact that they do not corrode. Currently, these fibers are produced from various polymers, including polyacrylate, polyamides, polyesters, polyethylene and other plastics (GLID et al. 2018, p. 12641–12650).

Fiber dosing value has a significant impact on the behavior of the concrete mix. The fibers can cause a reduced workability of the concrete mixture. Therefore, the entire mixture should be designed optimally and take care on the details. Due to the different shape and slenderness of the fibers, they can cause the formation of undesirable “hedgehogs” structure in a concrete mixture. To avoid it, the fibers should be added slowly to the concrete and mixed longer. After adding more than 4% of the weight of fibers to the concrete mixture, it can be concluded that these mixtures are already unstructured. Concrete mixtures

based on fibers can be only made in concrete containers, because such mixtures are almost impossible to pump (DINAKAR et al. 2013, p. 215–223, CENTONZE et al. 2015, p. 121–125, ZHANG et al. 2018, p. 57–65).

In conclusion, the use of fibers to the concrete has several advantages in reinforcement of the concrete composites, but due to the lack of the full experimental research of their influence on the properties of the composite in-depth study are necessary. Two types of recycled poly(propylene) fibers (with surface modification – grey fibers and without modification only after cutting process – green fibers) were used in the work and their influence on the final properties of ready concrete samples was analyzed.

## Materials and methods

This research results present the influence effect of two new poly(propylene) fibers (PP) from waste material on final properties of the composite.

The basic parameters of poly(propylene) fibers – morphology, thickness, circumference, length were analyzed by digital light microscope (Olympus LEXT OLS4100).

Concrete mixtures were fabricated by mechanical mixing process of portland cement, quartz sand, water and fibers in amount of 0.5 wt.% of cement. Fibers were added at the end of the process of mixing. The recipe includes three parts of aggregates with different grain size: 125–0.250, 0.250–0.500 and 0.500–1.000 mm. Mixing process was lasted for 5 min using mechanical mixer (100 RPM) in lab condition at 21°C and 50% of humidity. After that the concrete mixtures have been transported into steel forms and left for the curing process (28 days).

Setting time was measured used Vicat's machine. Slump cone test was calculated according to PN-EN 12350-2: 2011 standard.

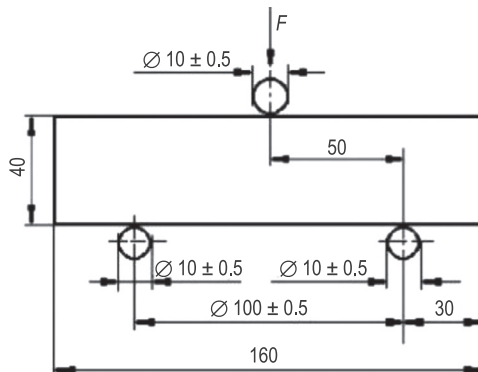


Fig. 1. Sample testing scheme of bending strength

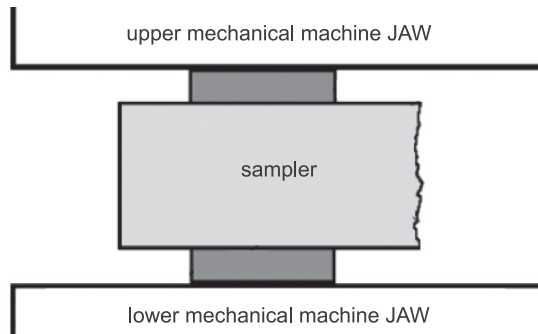


Fig. 2. Sample testing scheme of compressive strength

The measurement of the mechanical strength such as bending test and compressive strength was analyzed by Zwick machine on  $40 \times 40 \times 160$  mm samples after 1, 7, 14 and 28 days of curing process (Fig. 1, 2) using 10 samples for each test. After bending strength compressive strength was performed.

## Results and discussion

Figures 3 and 4 present the morphology of used fibers for concrete mixtures preparation. Presented images show two different structures of chosen fibers. One of them (grey) was modified into the extruder and the second one was without modification. The surface modification was used to increase the strength effect of the fibers addition. Irregular surface probably provides better anchoring effect into the concrete mass. After extruder modification the fibers exhibits more than usual stiffness. The second fiber comes from cutting process of waste

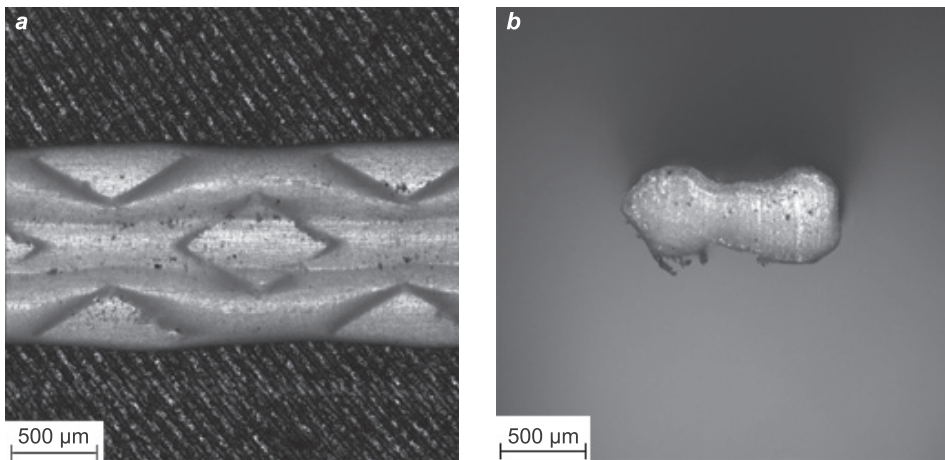


Fig. 3. Light microscope images of PP grey fibers: *a* – surface, *b* – cross section



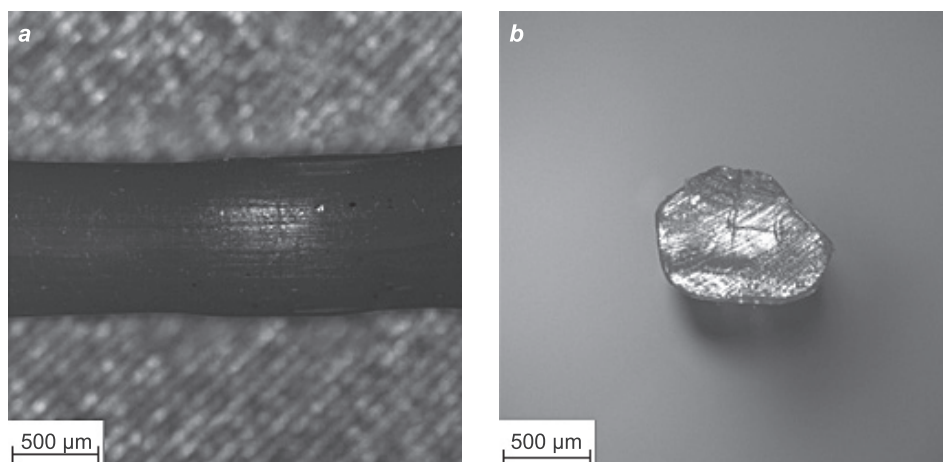


Fig. 4. Light microscope images of PP green fibers: *a* – surface, *b* – cross section

material. Both types of fibers are chemically identical, and come from with the same granulate product of PP. All tested fibers do not create agglomerates and they are easy to mix.

Table 1 shows the basic parameters of the researched fibers. Obtained results present that PP grey fiber exhibits higher values also in thickness and circumference parameters in comparison to the PP green fibers. The length of the both fibers is very similar, and it is approximately 31 mm.

Table 1

Basic properties of researched fibers			
Fiber	Thickness [ $\mu\text{m}$ ]	Circumference [ $\mu\text{m}$ ]	Length [mm]
PP grey	$1,146.6 \pm 5$	$566.5 \pm 5$	$31.2 \pm 0.5$
PP green	$888.9 \pm 5$	$485.2 \pm 5$	$30.9 \pm 0.5$

Distribution of initial and final setting time was presented on Figure 5. Significant changes between reference sample and sample with added new poly(propylene) fibers were not observed. The setting time is very similar for all samples. Initial time is almost 180 min. and final time is equal 240 min.

The results of the bending test were shown on Figure 6. After first day of curing process sample based on PP grey fibers exhibits the highest value of bending force – 2.5 kN. However, on the next day of measuring the highest values were noted for PP green samples. In the last day of testing (28 day) this sample indicate 33% more strength than PP grey samples and 72% more than reference sample.

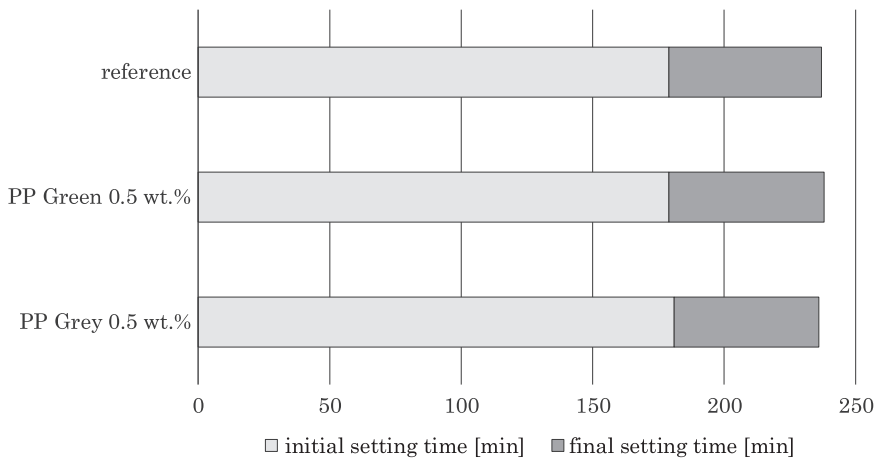


Fig. 5. Setting time distribution of tested mixtures

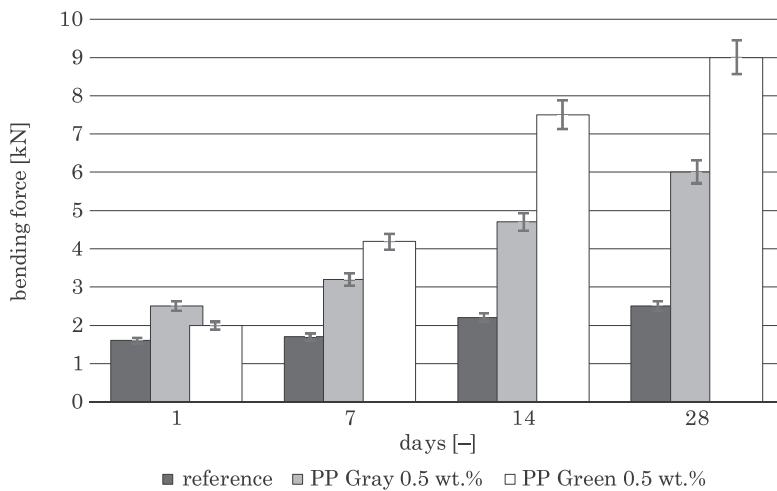


Fig. 6. Bending force distribution of concrete mixtures after 1, 7, 14 and 28 days of curing process

Compressive strength distributions of the researched samples were shown on Figure 7. It was noted that the PP green sample exhibits the highest values of compressive strength after all days of testing. Only measure after 7 days revealed the same value. The increasing effect was observed. On the 28 days of curing, compressive strength at level of 72 MPa was noted for PP green sample.

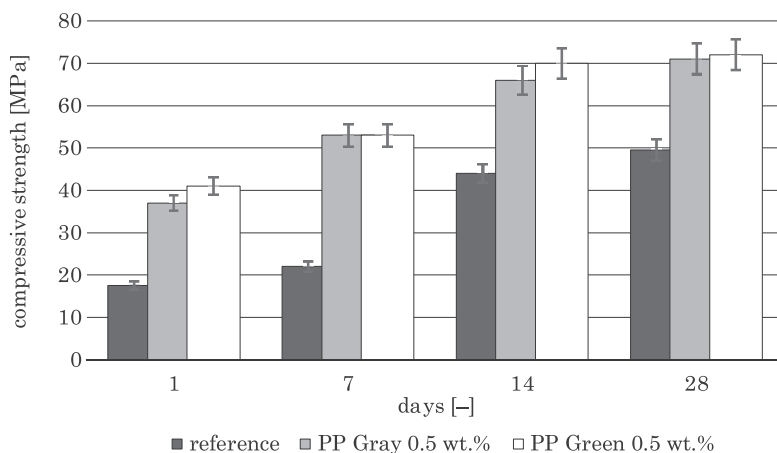


Fig. 7. Compressive strength distribution of concrete mixtures after 1, 7, 14 and 28 days of curing process

## Conclusions

According to the assumptions, the final influence of the addition of new poly(propylene) fibers from the waste materials to the matrix of concrete on the composite properties was proven and characterized in this paper. Addition of the fibers significantly improved the plasticity of the composite. Additionally, final compressive strength of the composite also increased in reference to pure concrete after all days of testing. Final mixture was not problematic in process of mixing and could be prepared in environment condition. This study proven that it is possible to produce new concrete composite using waste materials and obtain higher values of final properties. Additionally, replacement of a cement addition on the recycled waste fiber are more environmentally friendly and provide less of  $\text{CO}_2$  gases emitted (produced in the process of cement fabrication) in to the atmosphere.

## Acknowledgements

The paper has been prepared within the Statutory Research Work no. 934 in the Faculty of Civil Engineering and Geodesy in the Military University of Technology.

## References

- BANTHIA N., GUPTA R. 2006. *Influence of polypropylene fiber geometry on plastic shrinkage cracking in concrete*. Cement and Concrete Research, 36(7): 1263–1267.
- CENTONZE G., LEONE M., MICELLI F., AIELLO M., PETITO G. 2015. *Concrete reinforced with recycled steel fibres from scrap tires: a case study*. 8<sup>th</sup> International Conference Fibre Concrete, 3: 121–125.
- CHOUMANIDIS D., BADOGIANNIS E., NOMIKOS P., SOFIANOS A. 2016. *The effect of different fibres on the flexural behaviour of concrete exposed to normal and elevated temperatures*. Construction and Building Materials, 129(30): 266–277.
- DINAKAR P., SAHOO PRADOSH K., SRIRAM G. 2013. *Effect of Metakaolin Content on the Properties of High Strength Concrete*. International Journal of Concrete Structures and Materials, 7: 215–223.
- GLID M., SOBRADOS I., BEN RHAHEM H., SANZ J., AMARA AB. 2018. *Alkaline activation of metakaolin-silica mixtures: Role of dissolved silica concentration on the formation of geopolymers*. Ceramics International, 43: 12641–12650.
- KAKOOEI S., MD AKIL H., JAMSHIDI M., ROUHI J. 2012. *The effects of polypropylene fibers on the properties of reinforced concrete structures*. Construction and Building Materials, 27(1): 73–77.
- LIMA P.R.L., BARROS J.A.O., SANTOS D.J., FONTES C.M., LIMA J.M.F., TOLEDO FILHO R. 2016. *Experimental and numerical analysis of short sisal fiber-cement composites produced with recycled matrix*. European Journal of Environmental and Civil Engineering – in press.
- SMRKIĆ M.F., DAMJANOVIĆ D., BARIČEVIĆ A. 2017. *Application of recycled steel fibres in concrete elements subjected to fatigue loading*. Gradevinar, 69(10): 893–905.
- SONG P.S., HWANG S., SHEU B.C. 2005. *Strength properties of nylon- and polypropylene-fiber-reinforced concretes*. Cement and Concrete Research, 35(8): 1546–1550.
- ZHANG J., DING X.P., WANG Q., ZHENG X. 2018. *Effective solution for low shrinkage and low permeability of normal strength concrete using calcined zeolite particles*. Construction and Building Materials, 160: 57–65.



## ANALYSIS OF NATURAL FREQUENCY OF FLEXURAL VIBRATIONS OF A SINGLE-SPAN BEAM WITH THE CONSIDERATION OF TIMOSHENKO EFFECT

*Jerzy Jaroszewicz, Krzysztof Łukasiewicz*

Department of Production Management  
Faculty of Engineering Management  
Białystok University of Technology, Białystok, Poland

Received 14 February 2017, accepted 5 July 2018, available online 8 October 2018.

**Key words:** beam, boundary value problem, transversal vibration, Timoshenko effect, FEM, Cauchy function and characteristic series methods.

### Abstract

This paper presents general solution of boundary value problem for constant cross-section Timoshenko beams with four typical boundary conditions. The authors have taken into consideration rotational inertia and shear strain by using the theory of influence by Cauchy function and characteristic series. The boundary value problem of transverse vibration has been formulated and solved. The characteristic equations considering the exact bending theory have been obtained for four cases: the clamped boundary conditions; a simply supported beam and clamped on the other side; a simply supported beam; a cantilever beam. The obtained estimators of fundamental natural frequency take into account mass and elastic characteristics of beams and Timoshenko effect. The results of calculations prove high convergence of the estimators to the exact values which were calculated by Timoshenko who used Bessel functions. Characteristic series having an alternating sign power series show good convergence. As it is shown in the paper, the error lower than 5% was obtained after taking into account only two first significant terms of the series. It was proved that neglecting the Timoshenko effect in case of short beams of rectangular section with the ratio of their length to their height equal 6 leads to the errors of calculated natural frequency: 5%±12%.

## Introduction

Mechanical vibrations, in particular flexural vibrations are common in load-bearing structures, so designers have to perform calculations for dynamics to protect the structure from fatigue damage. Therefore, the dynamic calculations are important subject of interest in both engineering theory and practice. The initial stage of the calculation is to solve the boundary problem as results from vibrations which are determined by the natural frequencies and the corresponding mode shapes (TIMOSHENKO et al. 1985). In most cases, long an thin beams alone may be used to derive the equation of vibration by a simplified theory of Euler-Bernoulli. However, the experience shows that simplified theory can be applied for slender beams if one deals with higher vibration frequencies calculated. The development of industry and the construction of equipment particularly exposed to dynamic loads have caused the need to refine the technical calculation methods used in the classical strength of materials. In 1914, H. Lamb pointed out that even in the simplest case of an impact loaded beam, the elementary vibration equation given by Euler and Bernoulli is not true. This equation leads to a result showing that the impact of the suddenly applied load propagates at an infinite speed. In order to eliminate this error, the strength methods were abandoned and, as proposed by Timoshenko, corrections due to the Timoshenko effect were introduced (TIMOSHENKO 1971). They took into account the effect of transverse forces on bending and rotational inertia (Rayleigh correction). Table 1 shows the related exemplary results obtained by (SOLECKI, SZYMKIEWICZ 1964)

Table 1

The values of the first three frequencies for the above data in the case of a simply supported beam, with the consideration of Timoshenko effect

Frequency number $n$	$\bar{\omega}$ [rad/s] (without effect)	$\bar{\omega}$ [rad/s] (with effect)	Difference [%]
1	6	5.73	5
2	24	20.3	15
3	54	39.4	27

Although Timoshenko beam theory is much more complex than the fundamental one, it is much simpler than the solution of the three-dimensional theory of elasticity. The introduced correction caused a significant qualitative change in the beam vibration equation. It was possible, however, to capture the experimentally confirmed wave nature of the phenomenon, and with sufficient efficiency, it was also possible to discuss the results originating from the area of the wave fronts.

Figure 1 presents the dependence, drawn with the broken line, which was obtained by the Bernoulli theory, or with the dotted line, as stated by the refined theory. The continuous lines show the dependencies resulting from the exact solution of dynamic Lamé equations for a bar with the circular cross-section. The curves corresponding to the first three modes of vibrations were marked with digits I, II, III, respectively. The correlation of the curves shown in Figure 1 shows that the refined theory can provide satisfactory approximations for the lower orders of vibration. For large values, the  $k$ -divergence is rather important.

If wave number  $k \rightarrow \infty$  the exact value for velocity of surface Raleigh waves is  $c_R$ , whereas in Timoshenko theory the limit value is the velocity of longitudinal waves  $c_0$ .

For each fixed wave number, there are two phase speeds  $c_1, c_2$  which mainly correspond to the bending and cutting forms of the propagating waves. At  $k_2 R_2 \ll 1$ ;  $c_1 \approx k R c_0$ ;  $c_2 \approx \frac{c_t}{k R}$  hence  $c_1$  occurs with the velocity of bending waves, calculated on the base of the fundamental theory, with  $c_t$  being the velocity of deformation. The velocity  $c_2$  at  $k R \rightarrow 0$  increases to infinity (BOLOTIN 1979).

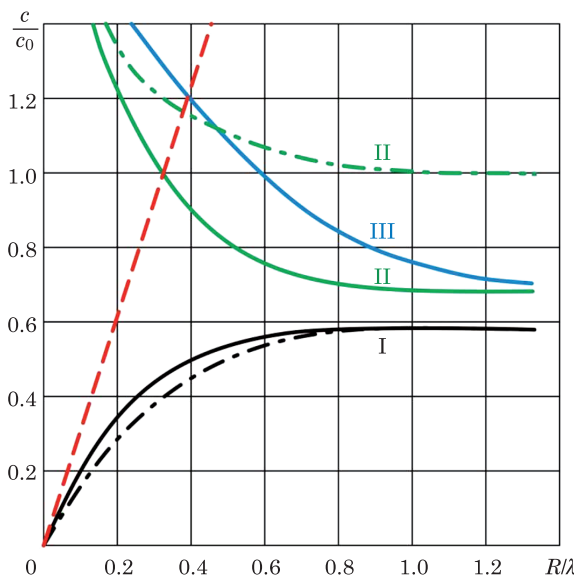


Fig. 1. Dependency of phase velocity of bending waves in rods on propagation coefficient, obtained by the use of a number of theories:  $c = k(EJ\rho F)^{1/2}$ ,  $R = (J/F)^{1/2}$ ,

$J, F$  – moment of inertia and the cross section area of the beam,  $\rho$  – denotes density of a material,  $E$  – Young modulus of elasticity  $\lambda$  – length of wave

Source: based on BOLOTIN (1979).

In the current work we solved the boundary problem of vibration bent for the four boundary conditions: both ends clamped, a simply supported end and the other clamped, soft simply supported on one end and hard simply supported on the other end, and the cantilever. To solve those problems, the Cauchy functions and series of characteristics developed under the personal guidance of prof. Zoryj were applied, for example in work (JAROSZEWICZ et al. 2004). Exact formulas for the coefficients of a number of characteristic were derived. Moreover, taking into account only the first two significant terms of the series resulted in error not exceeding 5%. On the basis of the derived formulas, numerical values of the coefficients of the short series were calculated for a reinforced beam with a rectangular profile of the ratio of length to height equal to 6. Disregarding the Timoshenko effect leads to the considerable calculation error. In order to calculate the fundamental frequency and the next two (the second and the third ones), double Bernstein estimates were used which appeared to be consistent with the exact values for the cantilever beam. The problem of impact of Timoshenko effect on vibrations of complex dynamic systems has been widely covered in literature, particularly in works (WU, CHIANG 2004, MAMANDI, KARGARNOVIN 2011, MOEENFARD et al. 2011, CHEN 2014, ZHANG et al. 2014, HSU 2016). Particular attention should be paid to publications (CAZZANI et al. 2016a, 2016b), in which the Timoshenko effect is evaluated for systems with variable mass and elastic parameters.

To solve the boundary problem, we use the methods of the Cauchy function and the method of characteristic series as an extension of Bernstein's spectral functions and double (lower and upper) estimators Bernstein-Kieropian, which were developed in 1977-2000 at the Lviv Polytechnic by prof. L. Zoryj and at the Bialystok University of Technology by prof. J. Jaroszewicz. It was shown that the above methods are effective for solving linear 4<sup>th</sup> order differential equations with fixed coefficients and variable coefficients containing singularities. Thanks to this method, the coupling conditions can be omitted, which increase the number of boundary conditions and increase the degree of the characteristic determinant.

The forms of characteristic equations proposed in the work allow to write the functional relationships between the frequency of the vibration form and the mass-elastic characteristics of the models. This allows not only to calculate the frequency and form of vibrations, but also to optimize and influence the formation of specific dynamic behaviors. For the construction of solutions of analogous differential equations, Bessel special functions were commonly used, which require solving complex systems of algebraic equations. Therefore, the proposed solution structure using the Cauchy function is much more effective and the characteristic equations are derived in the form of fast convergent power series of the frequency parameter. Double estimators give limits in which the exact frequency value is located using elementary functions. By deriving



a greater number of linear terms in the series, two or more frequencies can be determined without the need for numerically solving high order characteristic equations.

### The equation of flexural vibrations

In the case of load-bearing structures, like beams, in which height of cross section is larger than the span or length of the beam, and when higher natural frequencies are calculated, it is necessary to consider the influence of shear strain with regard to rotational inertia and shear, in literature known as the effect of Timoshenko (TIMOSHENKO 1971, THOMAS, ABBAS 1975).

Not considering these effects leads to the significant divergence with respect to calculations based on the Timoshenko theory (TIMOSHENKO et al. 1985, SOLECKI, SZYMKIEWICZ 1964).

For short beams, when calculating higher frequencies, when the wavelength of the deformation is comparable to the transverse beam dimensions, the technical theory of bending vibration, which does not take into account the shear and inertia of the rotation of the cross sections, results in large errors in calculations i.e. overestimates frequencies. The beam shape for the first mode of vibration is shown in Figure 2.

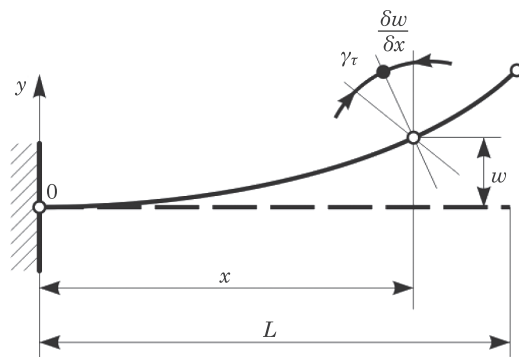


Fig. 2. The beam shape for the first mode of vibration:  $w$  – deflection of a beam,  $x$  – length of axis,  $L$  – length of beam,  $\frac{\delta w}{\delta x}$  – angle of bending,  $\gamma_\tau$  – angle of a cross-section  
Source: own elaboration.

Timoshenko beam is a sufficiently generalized calculation model for the studied load-bearing structure, with the consideration of influence of rotational angle and shear strain. The loading state of the element section of the beam is presented in Figure 3 and 4.

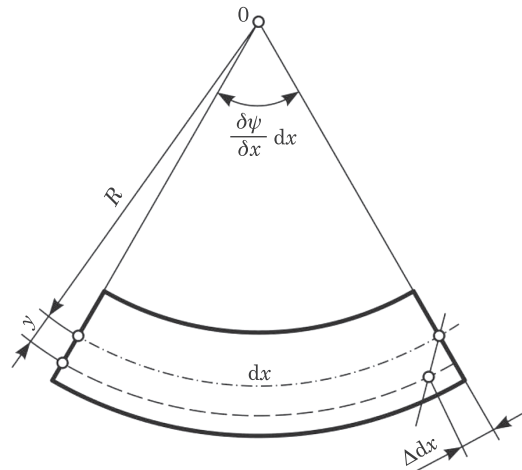


Fig. 3. Schematic diagram of the internal loading of the beam element resulting from the rotational inertia and inextensional strain:  $R$  – radius of element,  $y$  – length from neutral axis to section axis,  $dx$  – length of elementary element,

$\Delta dx$  – elongation,  $\psi$  – angle,  $\frac{\delta\psi}{\delta x} dx$  – elastic deformation

Source: based on VASYLENKO, ALEKSEJIUK (2004).

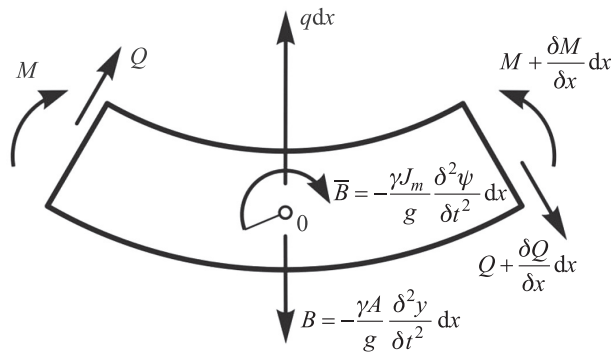


Fig. 4. Schematic diagram of loading of beam elements with respect to rotational inertia and non-dilatational strain:  $A$  – cross sectional area,  $M$  – moment of element bending,

$Q$  – shear power,  $B$  – inertia force,  $J_m$  – moment of inertia,  $g$  – acceleration of gravity,  $\gamma$  – mass density

Source: based on VASYLENKO, ALEKSEJIUK (2004).

For simplicity we assume that the beam performs the first bending mode of vibration for which (see: VASYLENKO, ALEKSEJIUK 2004):

$$\Theta = \frac{\partial w}{\partial x} + \gamma_t \tag{1}$$

Then, on the basis of Figure 2, we obtain:

$$Q = -KGF \left( \frac{\partial w}{\partial x} - \Theta \right) \tag{2}$$

where:

- $K = \frac{Jb}{FS}$  – the coefficient applied to establish shear deformation,
- $G$  – Kirchhoff module of elasticity,
- $J$  – a moment of cross section inertia,
- $F$  – cross section plane,
- $S$  – a moment of inertia of a part of the section located at one side of the axis of symmetry,
- $b$  – width of cross section in the neutral plane.

Taking into account the forces acting on the  $dx$  element, d'Alembert's inertial forces from the linear  $w$  and angular  $\Theta$  displacements of the sections (Fig. 2), we apply equations of dynamic equilibrium  $\sum Y = 0, \sum M_0 = 0$ . From these equations, rejecting infinitely small quantities of the second order, we obtain the following relations:

$$\frac{\partial Q}{\partial x} = q - \rho F \frac{\partial^2 w}{\partial t^2}, \quad \frac{\partial M}{\partial x} = Q + J_m \frac{\partial^2 \Theta}{\partial t^2} \tag{3}$$

Substituting equation (2) to (3), and taking into account known relations (VASYLENKO, ALEKSEJIUK 2004), we obtain the equations of forced vibrations of the elastic Timoshenko beam:

$$\begin{cases} \rho F \frac{\partial^2 w}{\partial t^2} - KGF \left( \frac{\partial^2 w}{\partial x^2} - \frac{\partial \Theta}{\partial x} \right) = q(x, t) \\ EJ \frac{\partial^2 \Theta}{\partial x^2} + KGF \left( \frac{\partial w}{\partial x} - \Theta \right) - J_m \frac{\partial^2 \Theta}{\partial t^2} = 0 \end{cases} \tag{4}$$

This work examines the method of analysis of transverse vibrations of the given beam with the use of Cauchy function and characteristic series (JAROSZEWICZ, ZORYJ 2000). Earlier, Jaroszewicz applied Cauchy function to analyze both static and dynamic problems of the beam systems (JAROSZEWICZ 1999, JAROSZEWICZ et al. 2014).

### Formulation of the boundary problem

From the equation (4), for a constant cross-section beam  $EJ = \text{const.}, GJ = \text{const.}, \rho F = \text{const}$  with  $q(x, t) = 0$ , we obtain the equation of motion of transverse free vibrations of load-bearing beam system, the elements of which are shown in Figure 1. This equation can be written (JAROSZEWICZ et al. 2004) in the form:

$$\rho F \frac{\partial^2 w}{\partial t^2} + EJ \frac{\partial^4 w}{\partial x^4} - \rho J \left(1 + \frac{E}{KG}\right) \frac{\partial^4 w}{\partial x^2 \partial t^2} + \frac{\rho^2 J}{KG} \frac{\partial^4 w}{\partial t^4} = 0 \tag{5}$$

where:

- $\rho$  – denotes density of a material,
- $E$  – Young modulus of elasticity,
- $w$  – a deflection of the beam,
- $x$  – the longitudinal beam coordinate,
- $t$  – time.

Determination of free frequencies needs solving the appropriate boundary value problem. Substitution of  $w = y \left(\frac{x}{l}\right) e^{\lambda t}$  with (5) and separation of two variables  $x$  and  $t$  give the differential equation with respect to  $x$ :

$$y^{IV} - \beta y'' - \delta y = 0, (0 \leq x \leq 1) \tag{6}$$

where:

- $\beta = \lambda^2 \rho J \left(1 + \frac{E}{KG}\right) l^2 (EJ)^{-1} = \lambda^2 A,$
- $\delta = -(EJ)^{-1} (\rho F \lambda^2 + \rho^2 \frac{J}{KG} \lambda^4) l^4 = -(\lambda^2 B + \lambda^4 C),$
- $w^2 = -\lambda^2$  – the second power of frequency.



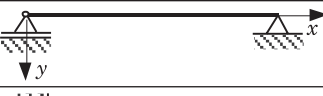
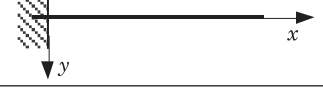
The formulas above contain the following symbols:

$$A = \frac{\rho l^2}{E} \left(1 + \frac{E}{KG}\right); B = \frac{\rho F l^4}{EJ}; C = \frac{\rho^2 l^4}{EKG} \tag{7}$$

Four cases of boundary conditions (Tab. 2), corresponding to the most frequently occurring supports of beams were analyzed of (JAROSZEWICZ et al. 2004).

Table 2

Four cases of boundary conditions

	$y(0) = y'(0) = 0$	$y(1) = y'(1) = 0$	(8)
	$y(0) = y''(0) = 0$	$y(1) = y'(1) = 0$	(9)
	$y(0) = y''(0) = 0$	$y(1) = y''(1) = 0$	(10)
	$y(0) = y'(0) = 0$	$y''(1) = y'''(1) = 0$	(11)

### The general solution

The general solution of equation (6) can be expressed in the following form (JAROSZEWICZ, ZORYJ 2000):

$$y = C_0\varphi + C_1\varphi' + C_2\varphi'' + C_3\varphi''' \tag{12}$$

in which the function  $\varphi(x, \beta, \delta)$  and its  $x$  derivatives are defined below, and where  $C_0, C_1, C_2, C_3$  denote arbitrary constants.

The Cauchy function appearing in the equation (12) is described with the formulas:

$$\varphi(x, \beta, \delta) = \sum_{K=0}^{\infty} \frac{J_K x^{K+3}}{(K+3)!} = \frac{1}{\mu^2 + \nu^2} \left( \frac{\text{sh} \mu x}{\mu} - \frac{\sin \nu x}{\nu} \right) \tag{13}$$

$$J_0 = 1, J_K = \beta J_{K-2} + \delta J_{K-4}, J_j = 0 \text{ for } j < 0$$

$$\mu^2 = \sqrt{\frac{1}{4}\beta^2 + \delta} + \frac{1}{2}\beta, \nu^2 = \sqrt{\frac{1}{4}\beta^2 + \delta} - \frac{1}{2}\beta$$

### Characteristic equations corresponding with the first three types of boundary conditions

Substitution of the form (12) in the boundary conditions (8) from Table 2, corresponding to the clamped-clamped beam, results in the following characteristic equation:

$$F = F(1, \beta, \delta) = ((\varphi')^2 - \varphi\varphi'')_{x=1} = 0 \tag{14}$$

where:

$$F = \sum_{n=0}^{\infty} (-1)^n 2^{2n+1} f_n(x, \beta) \delta^n \tag{15}$$

$$f(x, \beta) = \sum_{m=0}^{\infty} C_{2n+1+m}^{2n+1} \frac{\beta^m x^{4n+2m+4}}{(4n+2m+4)!} \tag{16}$$

$C_{2n+1+m}^{2n+1}$  – binominal coefficient.

Subsequent substitution of the general solution (12) in the conditions (9) yields the characteristic equations of a similar structure as before, on whose left side there is the following derivative of the function  $F$  from (15):

$$F'(1, \beta, \delta) = 0 \tag{17}$$

Subsequently, substitution of (12) in (10) leads to the following derivative on the left-hand side of (10):

$$F''(1, \beta, \delta) = 0 \quad (18)$$

Now we can construct function for boundary conditions (11) in power series form with respect to the coefficient  $\lambda^2$ . For this purpose, a few first functions can be calculated from (16):

$$\begin{aligned} f_0(x, \beta) &= \frac{x^4}{4!} + \frac{2x^6\beta}{6!} + \frac{3x^8\beta^2}{8!} + \dots \\ f_1(x, \beta) &= \frac{x^8}{8!} + \frac{4x^{10}\beta}{10!} + \frac{10x^{12}\beta^2}{12!} + \dots \\ f_2(x, \beta) &= \frac{x^{12}}{12!} + \frac{6x^{14}\beta}{14!} + \frac{21x^{16}\beta^2}{16!} + \dots \\ f_3(x, \beta) &= \frac{x^{16}}{16!} + \frac{8x^{18}\beta}{18!} + \frac{36x^{20}\beta^2}{20!} + \dots \\ f_4(x, \beta) &= \frac{x^{20}}{20!} + \frac{10x^{22}\beta}{22!} + \dots \end{aligned} \quad (19)$$

and a few first terms of the series (15) are:

$$F = 2f_0 - 2^3 f_1 \delta + 2^5 f_2 \delta^2 - 2^7 f_3 \delta^3 + \dots \quad (20)$$

The right-hand side of the relation (20) can be written in a form of a series:

$$\Delta \equiv a_0 + a_1 \lambda^2 + a_2 \lambda^4 + a_3 \lambda^6 + \dots \quad |_{x=1} = 0 \quad (21)$$

presented as a characteristic series, also named the Bernstein spectral function of the formulated boundary value problem. The characteristic equation (21) in the form of the power series in relation to the frequency parameter is obtained by substituting the general form of equation (12) to the boundary conditions from Table 2, equating equations of the system of four algebraic equations to zeros, and then using the conditions for non-zero values for integration constants  $C_0, C_1, C_2, C_3$ .

Formulas for the first four terms of a series (16) for the example presented in Table 2 have been determined by using relations (17)÷(20):

$$a_0 = \frac{2}{4!}, \quad a_1 = \frac{4}{6!}A + \frac{2^3}{8!}B \tag{22}$$

$$a_2 = \frac{3 \cdot 2}{8!}A^2 + \frac{2^3 \cdot 4}{10!}AB + \frac{2^3}{8!}C + \frac{2^5}{12!}B^2$$

$$a_3 = \frac{4 \cdot 2}{10!}A^3 + \frac{2^3 \cdot 10}{12!}A^2B + \frac{2^3 \cdot 4}{10!}AC + \frac{2^5 \cdot 6}{14!}AB^2 + \frac{2^6}{12!}BC + \frac{2^7}{16!}B^3$$

$$a_4 = \frac{5 \cdot 2}{12!}A^4 + \frac{2^3 \cdot 20}{14!}A^3B + \frac{2^3 \cdot 10}{12!}A^2C + \frac{2^5 \cdot 21}{16!}A^2B^2 + \frac{2^6 \cdot 6}{14!}ABC + \dots$$

where  $A, B, C$  are constants defined with (7).

The above formulas (22), correspond to a clamped-clamped support – the case (8). For the cases (9) and (10), the formulas for subsequent coefficients of the characteristic series (21) can be written, bearing in mind that  $F'(1, \beta, \delta) = 0$  in the case (9) and  $F''(1, \beta, \delta) = 0$  in the case (10).

Having obtained coefficients (22), Bernstein-Keropian double (upper and lower) estimators have been applied to calculate base frequency and the next two (the second and the third ones). Results of the calculation are presented below, in section 6. It should be noted here that the first and second frequencies have been received with a great accuracy, and the third and fourth ones are determined with approximate values. Approximate values may be enhanced by means of iteration method with use of formula (12) and the exact expression for the function (15):

$$F = \frac{1}{(\mu^2 + \nu^2)^2} \left[ (\mu^2 + \nu^2) \frac{\text{sh}\mu \sin \nu x}{\mu\nu} + 2(1 - \text{ch}\mu x \cos \nu x) \right] \tag{23}$$

### Characteristic equations in the case of cantilever beam boundary conditions

In case of cantilever beam with Timoshenko effect taken into account, for which boundary conditions are in the form (11) (Tab. 2), the characteristic equation can be obtained in the following form:

$$1 - \delta F(1, \beta, \delta) = 0 \tag{24}$$

which, by substituting  $\delta$  in (24) and accounting for (7), reads:

$$1 + (\lambda^2 B + \lambda^4 C) \cdot F(1, \beta, \delta) = 0 \tag{25}$$

Then, consideration of (12) leads to the following coefficients of characteristic series:

$$\begin{aligned}
 a_0 &= 1; \quad a_1 = \frac{2}{4!}B; \quad a_2 = \frac{2}{8!}B^2 + \frac{4}{6}AB + C \\
 a_3 &= \frac{2^5}{12!}B^3 + \frac{3 \cdot 2}{8!}A^2B + \frac{2^3 \cdot 4}{10!}AB^2 + \frac{2^3}{8!}CB + \frac{4}{6!}AC + \frac{2^3}{8!}BC \quad (26) \\
 a_4 &= \frac{2^7}{16!}B^4 + \frac{4 \cdot 2}{10!}A^3B + \frac{2^3 \cdot 10}{12!}A^2B^2 + \frac{2^6}{10!}ABC + \frac{2^5 \cdot 6}{14!}AB^3 + \frac{2^5 \cdot 3}{12!}B^2C + \\
 &+ \frac{3 \cdot 2}{8!}A^2C + \frac{2^3}{8!}C^2 \dots
 \end{aligned}$$

The final form of equation (25) is received by means of transformation of the expressions (26)

$$1 - \delta F(x, \lambda) = 0 \quad (27)$$

where:

$$F(x, \lambda) = \sum_{n=0}^{\infty} \lambda^{2n} \left\{ \sum_{j=0}^{n/2} C^j \sum_{m=j}^{n-j} 2^{2m+1} \frac{x^{2n+2m+2j+4}}{(2n+2m+2j+4)!} C_{m+n-j+1}^{2m+1} C_m^j A^{n-m-j} B^{m-j} \right\} \quad (28)$$

The result in the form corresponding to the case without Timoshenko effect and values of estimators is not difficult to obtain from formulas (27):

$$a_0 = 1; \quad a_1 = \frac{2}{4!}B; \quad a_2 = \frac{2^3}{8!}B^2 \quad (29)$$

$$\sqrt{\frac{EJ}{ml^4}} 1.8749 < \omega_1 < 1.8751 \sqrt{\frac{EJ}{ml^4}} \quad (30)$$

Values of coefficients of base frequencies which were calculated on base of Bernstein estimators [1] are in agreement with the exact values calculated by means of Krylov-Prager (THOMAS, ABBAS 1975) function for cantilever.

Calculation results of base frequency for four cases of supports, according to the proposed method

Table 3, presented below, contains formulas for the first three terms of a series without Timoshenko effect.

The application of Cauchy influence function and characteristic series to the analysis of the transverse vibration of short beams gave results in the form of characteristic power series (21) for which closed formulas for the first four terms of series (22) and (26) can be formulated. The calculations of frequency



Table 3

Final formulas for the first three terms of a series without Timoshenko effect

Boundary conditions from Table 2	$a_0$	$a_1$	$a_2$
(8)	$\frac{2}{4!}$	$\frac{2^3}{8!}B$	$\frac{2^5}{12!}B^2$
(9)	$\frac{2}{3!}$	$\frac{2^3}{7!}B$	$\frac{2^5}{11!}B^2$
(10)	$\frac{2}{2!}$	$\frac{2^3}{6!}B$	$\frac{2^5}{10!}B^2$
(11)	1	$\frac{2}{4!}B$	$\frac{2^3}{8!}B^2$

were adjusted for the first three terms of the series. On the basis of the simplest Bernstein estimators, and by the use of previously listed formulas, the base frequency can be calculated (BERNSTEIN, KIEROPIAN 1960):

$$\frac{a_0}{\sqrt{a_1^2 - 2a_0a_2}} < \omega_1^2 < \frac{2a_0}{a_1 + \sqrt{a_1^2 - 4a_0a_2}} \tag{31}$$

If one knows  $a_3$  and  $a_4$  and the coefficients (22) and (26) for the frequency of equation (21), the plate first three frequencies can be estimated and the approximate value of the fourth frequency can be determined. First, let us calculate the following numbers:

$$B_1 = \frac{a_1}{a_0} = \frac{1}{60}, \quad B_2 = \left(\frac{a_1}{a_0}\right)^2 - 2\frac{a_1a_2}{a_0^2} = 0.0001786 \tag{32}$$

and the ratio:

$$\frac{B_2}{B_1^2} = 0.64288 \tag{33}$$

for which the corresponding results are given in BERNSTEIN, KIEROPIAN (1960, Tab. 21, p. 236). The following formulas are used:

$$\omega_i = \gamma_i \frac{1}{R^2} \sqrt{\frac{D_0}{\rho h_0}}, \quad (i = 1, 2, 3) \tag{34}$$

$$(\gamma_i)_- = \sqrt[4]{\frac{\varphi_i}{B_i}}, \quad (\gamma_i)_+ = \sqrt[4]{\frac{\beta_i}{B_1}}, \quad (i = 1, 2, 3) \tag{35}$$

$$\gamma_4 \approx \sqrt[4]{\frac{\psi}{B_1}} \tag{36}$$

Expression (36) defines the approximate estimate of the fourth eigenvalue parameter according to Bernstein-Kieropian tables. Having the first 3 coefficients of equation (21)  $a_0, a_1, a_2$  calculated, one can determine the estimators of the first three vibration frequencies and approximate the fourth one. Bernstein and Kieropian developed formulas for estimators of higher frequencies and placed them in tables of relations between them. When calculating the ratio (33), we read on the basis of [1] the values:  $\varphi_1, \varphi_2, \varphi_3, \beta_1, \beta_2, \beta_3$  and  $\psi$  and then we calculate the upper and lower estimators of the higher frequencies.

Taking relations (32)–(36), and substituting  $a_0 = 1$ , and  $a_1$  and  $a_2$  from (22) into these relations, we obtain:

$$\begin{aligned} 8.64 < \gamma_1 < 8.85 \\ 10.06 < \gamma_2 < 20.08 \\ 31.61 < \gamma_3 < 52.56 \\ \gamma_4 \approx 66.61 \end{aligned} \tag{37}$$

Coefficients of the characteristic series of the present beam without Timoshenko effect, manifested by zero values  $A$  and  $C$ , are presented in Table 3. To calculate the subsequent frequencies, Bernstein tables must be applied (BERNSTEIN, KIEROPIAN 1960).

The calculation results of the lower and upper estimators of the base frequency, without Timoshenko effect, conducted by using symbols from Table 3, correspond to the exact values (TIMOSHENKO 1971, THOMAS, ABBAS 1975, SOLECKI, SZYMKIEWICZ 1964) and they are listed in Table 4.

The results of calculation of the lower and upper estimators of the base frequency are obtained with Timoshenko effect for concrete beam with a rectangular cross-section, in which: the ratio of length to cross-sectional height is:

Table 4

Values of estimators for the base frequency in the case of four support without Timoshenko effect

Boundary conditions	Low estimator $\frac{1}{\pi} \sqrt{\frac{\rho Fl^4}{EJ}} (\omega_1)_-$	High estimator $\frac{1}{\pi} \sqrt{\frac{\rho Fl^4}{EJ}} (\omega_1)_+$	Exact value $\frac{1}{\pi} \sqrt{\frac{\rho Fl^4}{EJ}} (\omega_1)$
(8)	4.720	4.732	4.730
(9)	3.818	3.924	3.927
(10)	3.140	3.143	$\pi$
(11)	1.802	1.875	1.870

$l/h = 6$ , Young modulus and Kirchoff modulus relationship reads  $E/G = 2.5$ , and shape of the section is  $K = Jb/FS = 2/3$ , the area of cross-section equals:  $F = b \cdot h = 0.5 \text{ m}^2$ , the moment of inertia of a cross-section is:  $J_x = bh^2/12 = 0.042 \text{ m}^4$ ,  $S$  – the first moment of the section area located on one side of the axis neutral to this axis,  $\rho = 24,000 \text{ N s}^2/\text{m}$  – the density of the material. Parameters  $A, B, C$ , calculated with formulas (7) are as follows:  $A = 0.029882 \text{ 1/s}^2$ ,  $B = 2.718 \text{ 1/s}^2$ ,  $C = 0.000148 \text{ 1/s}^4$ . These results for geometrical and material exemplary parameters are listed in Table 5. They correspond to the calculation results presented in the work (SOLECKI, SZYMKIEWICZ 1964).

Table 5

Values of the first three coefficients of the characteristic series for the base frequency for the cases from Table 2, without Timoshenko effect.

Boundary conditions	$a_0$	$a_1 \cdot 10^{-4}$	$a_2 \cdot 10^{-6}$	$\tilde{\omega}_1$ [rad/s]	$(\omega_1)_+$ [rad/s]	$(\omega_1)_-$ [rad/s]	$(\omega_1)_{SR}$ [rad/s]
(8)	1/12	5.4	0.5	12.43	13.65	13.51	13.58
(9)	1/3	43.14	5.9	8.79	8.96	8.87	8.91
(10)	1	302	6.5	5.99	5.58	5.56	5.57
(11)	1	2264	1465	2.11	2.13	2.13	2.13

Table 6

Values of the first three coefficients of the characteristic series for the base frequency for the cases from Table 2, with Timoshenko effect

Boundary conditions	$a_0$	$a_1 \cdot 10^{-4}$	$a_2 \cdot 10^{-6}$	$\tilde{\omega}_1$ [rad/s]	$(\omega_1)_+$ [rad/s]	$(\omega_1)_-$ [rad/s]	$(\omega_1)_{SR}$ [rad/s]
(8)	1/12	7.05	1.41	11.87	13.57	12.68	13.13
(9)	1/3	57.01	6.3	8.16	8.25	8.22	8.24
(10)	1	456	7.03	5.22	5.31	5.23	5.27
(11)	1	2264	1995	2.09	2.05	2.06	2.06

Table 6 presents the results of the calculations with Timoshenko effect and Bernstein double estimators by formulas (22) for the boundary conditions (8), then by (26) for the conditions (11), and the results on the base of biquadratic equation (32) for the case (10). The results of calculations for a rough Dunkerley estimator for cases (8), (10) and (11) were based on the formula (JAROSZEWICZ, ZORYJ 2000):

$$\tilde{\omega}_1 \approx \frac{1}{\sqrt{a_1}} \tag{38}$$

where  $\tilde{\omega}_1$  is the course value of the basic frequency estimate, calculated on the basis of the first part of the series  $a_1$ .

For the case of a free-ends beam without Timoshenko effect, on the base of (32) and Table 3 formulas for the cases (8)÷(11) can be formulated:

$$\tilde{\omega}_1 \approx \frac{1}{\sqrt{B/420}}, \tilde{\omega}_1 \approx \frac{1}{\sqrt{B/720}}, \tilde{\omega}_1 \approx \frac{1}{\sqrt{B/90}}, \tilde{\omega}_1 \approx \frac{1}{\sqrt{B/12}} \quad (39)$$

## Numerical analysis

For comparison purposes, the calculations of the distribution and values of concentrated strain have been calculated with the use of FEM. Autodesk Inventor 2015 software equipped with NASTRAN module has been applied. The comparison has only related to natural frequency distribution determined analytically using the relationship (31) and (38), so the focus was on the calculation with linear behavior of the material. Calculations covered four cases of beam support shown in Table 2. The dimensions of the beam, material constants and boundary conditions were assumed in the same way as in the analytical studies. Due to the simple shape of the beam, the problem was modeled as a spatial one, adopting a standard mesh that uses 10-node elements. Table 7 shows information on the developed mesh for the studied beam.

Calculations of the percentage difference in the results for different types of beam supports and calculation methods have been conducted according to the formula (40), and these values are given in Table 8.

$$\Delta s = \left| \frac{\omega_{sr}^{ANL} - \omega^{MES}}{\omega_{sr}^{ANL}} \right| \cdot 100\% \quad (40)$$

where:

$\omega_{sr}^{ANL}$  – analytically determined natural frequency,  
 $\omega^{MES}$  – FEM-determined natural frequency.

Table 7

Mesh parameters	
Type of mesh	Parabolic tetrahedral
Max. element Growth Rate	1.5
Refinement Ratio	0.2
Min./Max. Trangle Angle	20/30 deg
Upper Jacobian Ratio Bound	16 points
Size	200 mm
Tolerance	0.0356 mm
Quality	high
Elements	2,600
Nodes	3,851

Table 8

Percentage values of difference in results for FEM and analytical method

Boundary conditions	Values $\omega^{MES}$ [rad/s]		Difference in results without Timoshenko effect [%]		Difference in results with Timoshenko effect [%]	
	1 <sup>st</sup> freq.	2 <sup>nd</sup> freq.	1 <sup>st</sup> freq.	2 <sup>nd</sup> freq.	1 <sup>st</sup> freq.	2 <sup>nd</sup> freq.
(8)	12.87	29.96	5.28	8.71	2.04	4.23
(9)	8.53	23.41	4.31	7.76	3.47	3.12
(10)	5.41	21.541	2.88	6.48	2.65	5.08
(11)	2.08	11.78	2.15	5.37	1.17	2.81

### Conclusion

The characteristic equations which have been obtained in this paper and final formulas resulting from them, provide the mathematical safeguard for calculation of the lower and upper estimators of the base frequencies of short beams with the rotational inertia and non-dilatational strain taken into account, and with the most common boundary conditions found in engineering practice.

Application of the Cauchy function and the corresponding characteristic series for analysis of transverse vibrations of short beams has demonstrated efficiency of these methods in terms of accuracy and in the ability of formulating functional relations between the mass and elasticity parameters of beams for an arbitrary section, arbitrary relationship of longitudinal and non-dilatational elasticity module, and arbitrary natural frequencies.

Consideration of first three terms of series allows for receiving convergence to the analytical solution results of the fundamental frequency coefficients, with accuracy to three decimal digits.

Formulas, proposed in this paper can be particularly useful for preliminary engineering calculations as well as for didactic objectives in the dynamics of short structural elements, in which application of simplified technical bending theory leads to unacceptable errors in natural frequency calculations, especially for higher frequencies, starting from the second one.

FEM – Autodesk NASTRAN environment allows for precise forecasting of a beam’s natural frequencies. Frequencies whose values are, for the most part, within the specified analytical considerations range. It can be observed that the results obtained in the FEM environment show lower percentage differences with respect to the analytical considerations when the Timoshenko effect is taken into account.

## Acknowledgement

The research was performed within S/WZ/1/2015 project financed by the Ministry of Science and Higher Education.

## References

- BERNSTEIN S.A., KIEROPIAN K.K. 1960. *Calculation of Frequency of Bar Systems by Means of Spectral Function*. Goststrojtechizdat, 281.
- BOLOTIN V.V. 1979. *Handbook "Vibration in Technique"*, in 6 V. Mashinostroenie. Moscow.
- CAZZANI A., STOCHINO F., TURCO E. 2016a. *On the whole spectrum of Timoshenko beams*. Part I: *A theoretical revisitaton*. *Zeitschrift für angewandte Mathematik und Physik ZAMP*67:24 (doi: 10.1007/s00033-015-0592-0).
- CAZZANI A., STOCHINO F., TURCO E. 2016b. *On the whole spectrum of Timoshenko beams*. Part II: *Further applications*. *Zeitschrift für angewandte Mathematik und Physik ZAMP*67:25 (doi:10.1007/s00033-015-0596-9).
- CHEN W.R. 2014. *Effect of local Kelvin-Voigt damping on eigen frequencies of cantilevered twisted Timoshenko beams*. *Procedia Engineering*, 79: 160–165.
- HSU Y.S. 2016. *Enriched finite element methods for Timoshenko beam free vibration analysis*. *Applied Mathematical Modelling*, 40: 7012–7033.
- JAROSZEWICZ J. 1999. *The effect of non-homogenous material properties on transverse vibration of elastic cantilever*. *International Applied Mechanics*, 35(6): 103–110.
- JAROSZEWICZ J., ZORYJ L. 2000. *Investigation of axial loads on transverse vibrations of vertical cantilevers of variable parameters*. *International Applied Mechanics*, 36(9): 1242–1251.
- JAROSZEWICZ J., ZORYJ L., PUCHALSKI W. 2004. *Natural frequencies of vibration of flexible elements of load-bearing structures taking into account the Timoshenko effect*. *Materials of the 3<sup>rd</sup> Scientific and Practical Conference "Energy in Science and Technology"*, Suwalki, p. 57–68.
- JAROSZEWICZ J., ŻUR K.K., DRAGUN Ł. 2014. *The influence function method in analysis of bending curve and relations of elastic supports of beam with variable parameters*. *Journal of Theoretical and Applied Mechanics*, 52(1): 247–255.
- MAMANDI A., KARGARNOVIN M.H. 2011. *Dynamic analysis of an inclined Timoshenko beam traveled by successive moving masses/forces with inclusion of geometric nonlinearities*. *Acta Mechanica*, 218: 9–29.
- MOENFARD H., MOJAHEDI M., AHMADIAN M.T. 2011. *A homotopy perturbation analysis of nonlinear free vibration of Timoshenko microbeams*. *Journal of Mechanical Science and Technology*, 25(3): 557–565.
- SOLECKI R., SZYMKIEWICZ J. 1964. *Rod and surface systems dynamic calculations*. Arkady, Warszawa.
- THOMAS J.B., ABBAS B. 1975. *Finite element model of dynamic analysis of Timoshenko beam*. *Journal Sound and Vibration*, 41(3): 291–299.
- TIMOSHENKO S.P. 1971. *The stability of rods, plates and shells*. Science, Moscow.
- TIMOSHENKO S.P., JANG D.H., UIVER U. 1985. *Vibration in engineering applications*. Ma inostrojenije, Moscow, p. 472.
- VASYLENKO M.W., ALEKSEJIUK O.M. 2004. *Vibration theory and motion stability*. Higher School, Kiev.
- WU J.S., CHIANG L.K. 2004. *Free vibration of a circularly curved Timoshenko beam normal to its initial plane using finite curved beam elements*. *Computers and Structures*, 82: 2525–2540.
- ZHANG B., HE Y., LIU D., GAN Z., SHEN L. 2014. *Non-classical Timoshenko beam element based on the strain gradient elasticity theory*. *Finite Elements in Analysis and Design*, 79: 22–39.



Quarterly peer-reviewed scientific journal

ISSN 1505-4675  
e-ISSN 2083-4527

**TECHNICAL SCIENCES**

Homepage: [www.uwm.edu.pl/techsci/](http://www.uwm.edu.pl/techsci/)



## ASSESSMENT OF COMFORT OF USE OF FOOTBRIDGES

*Marek Pańtak, Kinga Marecik*

Chair of Bridges and Tunnels Construction  
Institute of Building Materials and Structures  
Faculty of Civil Engineering  
Cracow University of Technology

Received 5 May 2017, accepted 30 September 2018, available online 8 October 2018.

**Key words:** comfort, footbridges, vibrations, dynamics, serviceability limit state.

### Abstract

To assess the comfort of use of the structures designed for human use during its vibrations it is necessary to know the requirement of the comfort criteria for the specific type of the structure. In the paper the issue of evaluation of the footbridges vibrations acceptability along with proposal of comfort criteria for the footbridges elaborated on the basis of survey researches were presented. The proposal of the vibration comfort criteria taking into account frequency of vibrations occurrence (frequent, rare and exceptional events) were characterized and compared with propositions of other authors, standards and recommendations.

### Introduction

Constant progress in material engineering affects the design principles of building structures. The structural materials getting better resistance parameters enable to design a new structures with greater spans and smaller dimensions of cross sections of the structural elements. The contemporary footbridges become lighter and longer than older one. They have smaller vertical and horizontal stiffness, smaller mass and lower values of damping parameters. Because of that they can be susceptible to different dynamic actions. An important type

---

Correspondence: Marek Pańtak, Katedra Budowy Mostów i Tuneli, Wydział Inżynierii Lądowej, Politechnika Krakowska im. Tadeusza Kościuszki, ul. Warszawska 24, 31-155 Kraków, e-mail: [mpantak@pk.edu.pl](mailto:mpantak@pk.edu.pl)

of dynamic loads of footbridges are loads generated during human movement. These dynamic loads may have various sources of origin e.g. forces generated during walking, running, jumps, squats or other rhythmic and choreographic activities. Fundamental vibration frequencies of the light-weight footbridges are often in the frequency range of human action 1.4–3.4 Hz (BACHMANN, AMMANN 1987, PAŃTAK 2007).

Dynamic response of these footbridges, correctly designed for variable actions accepted in accordance with PN-EN 1991-2:2007 (2007) i.e. uniformly distributed crowd loading including the dynamic amplification effects and treated in design as a static load, can exceed established vibrations limits during vibrations caused by dynamic loads generated by moving users of the footbridge (i.e. changing in time ground reaction forces) especially in the case of occurrence of resonant vibrations of the structure. It should be clearly noted that variable action of the crowd including dynamic amplification effects used as a static load cannot be assumed as a substitute of pedestrian dynamic actions (see PN-EN 1991-2:2007 2007, Chapter 5.1 (4) and 5.7). The static load does not allow to determine vibration amplitudes defined as a vibration acceleration and should not be treated as a guarantor of fulfilment of the requirement of vibration comfort criteria.

In the case of high dynamic susceptibility of the footbridge, users can experience unpleasant vibrations of the structure (especially in cases of light-weight steel footbridges with small damping). It should be noted that vibrations are an important limit state in the design of footbridges.

In order to check the requirements of limit state of vibrations the amplitudes of the forced vibrations of the structure should be calculated and compared with permissible vibrations amplitudes specified in the comfort criteria. The comfort criteria should be developed taking into account a number of parameters affecting the human perception of vibrations.

The main parameters determining the human sensitivity to vibrations are: position of the body (sitting, standing, lying), direction of transmission of the vibrations onto the human spine (vertical, horizontal), frequency response of the vibrations, human activity (resting, walking, running), age and sex, time of the day (day, night), duration of the vibrations, frequency of occurrence and nature of the vibrations (continuous, intermittent, impulse) as well as predictability of the vibrations and degree of habituation to the vibrations (BACHMANN, AMMANN 1987, FLAGA 2002).

Fundamental parameters determining the intensity of human perception of vibrations are: vibrations amplitude, frequency response of the vibrations, direction of the vibrations, vibrations impact time (exposure time), repeatability of the vibrations (FLAGA 2002).

The limit values of vibrations are often defined as a value of accepted acceleration of vibrations in function of frequency and duration of the vibrations for three orthogonal directions. In the case of stochastic vibrations the



limit value of acceleration of vibrations is assumed as a root-mean-square (*rms*) value of acceleration of vibrations  $a_{rms}$  calculated for defined averaging time. For harmonic vibrations the limit value of acceleration of vibrations is assumed as a peak value of acceleration of vibrations  $a_{max}$  (without averaging of the value of acceleration).

## Comfort criteria for footbridges – review of recommendations

Different recommendations of comfort criteria for the assessment of comfort of use of the footbridges can be found in several documents: ISO 10137... (2007), PN-EN 1990:2004/A1 (2008), *Footbridges – Assessment of vibrational behaviour...* (2006) and in older ones: *Steel, Concrete and Composite...* (1978), BACHMANN, AMMANN (1987), GRUNDMANN et. al. (1993), PAŃTAK (2007), PAŃTAK et. al. (2012).

The comfort criteria presented in ISO 10137... (2007) were established with two assumptions: minimum adverse comments of the population subjected to vibrations, vibrations do not unduly alarm of the footbridge users. The criteria were defined in the form of two base curves with appropriate multipliers depending on the type of the structure. The base curves were defined for two direction of the vibration: vertical and horizontal.

According to ISO 10137... (2007) the acceptable acceleration of vibrations for footbridges in vertical direction should not exceed levels obtained by multiplying the base curve for the vertical direction by factor of 60, except situations where one or more persons standing still on the walkway, in these cases a multiplier of 30 should be applicable (Fig. 1a). In cases of horizontal vibrations level of vibrations should not exceed 60 times the base curve for the horizontal direction (Fig. 1b). Limit values of vibrations were defined in terms of root-mean-square (*rms*) value of acceleration. For the calculation of (*rms*) values of the acceleration an averaging time of 1 s is recommended.

Another document containing recommendations for assessing of comfort of use of the footbridges is a design standard (PN-EN 1990:2004/A1 2008). The comfort criteria presented in PN-EN 1990:2004/A1 (2008) are defined in terms of maximum acceptable acceleration  $a_{max}$  (peak acceleration of vibrations). The recommended acceptable maxima of acceleration  $a_{max}$  are:  $a_{max,v}=0.7$  m/s<sup>2</sup> for vertical vibrations,  $a_{max,h}=0.2$  m/s<sup>2</sup> for horizontal vibrations due to normal use and  $a_{max,h}=0.4$  m/s<sup>2</sup> for horizontal vibrations in case of vibration induced during exceptional crowd conditions. It was pointed out that other criteria may be defined as appropriate in the National Annex.

Based on dynamic investigations and analyses of numerous footbridges in *Steel, Concrete and Composite...* (1978) the upper limit of tolerable acceleration for footbridges with natural vertical vibration frequency  $f \leq 5.0$  Hz

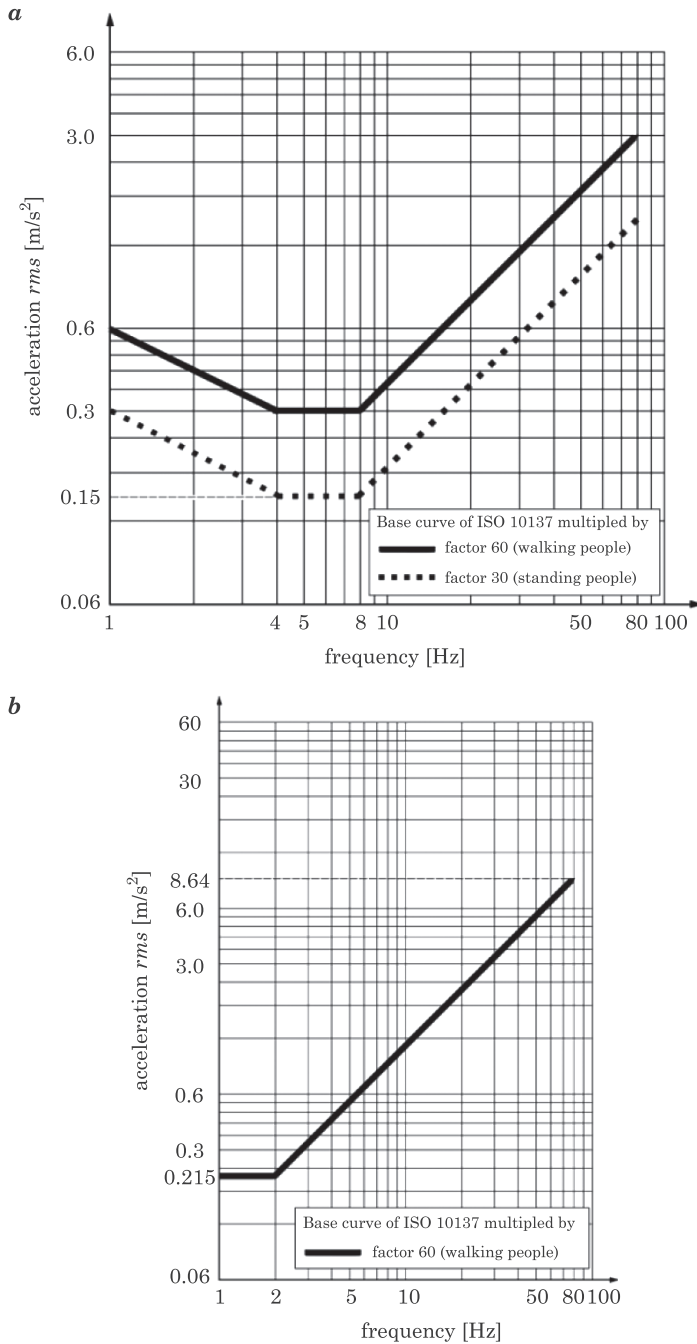


Fig. 1. The comfort criteria for footbridges according to ISO 10137 (2007) for: *a* – vertical vibrations, *b* – horizontal vibrations (side to side and forward to reverse)  
 Source: own elaboration.

was specified as  $a_{\max} = 0.5 \cdot f^{0.5}$  m/s<sup>2</sup> (where  $f$  – vibration frequency of the structure). For instance, during vertical vibrations of the structure with frequency  $f = 1.7\text{--}2.3$  Hz the range of tolerable acceleration of vibrations is  $a_{\max} = 0.65\text{--}0.75$  m/s<sup>2</sup>. In *Steel, Concrete and Composite...* (1978) there are no any recommendations for acceptable level of acceleration of horizontal vibrations.

Taking into account own experiences (BACHMANN, AMMANN 1987) proposed the permissible levels of peak acceleration of vibrations for pedestrian structures  $a_{\max}$  in the range of  $0.5\text{--}1.0$  m/s<sup>2</sup> for vertical vibrations and  $0.1\text{--}0.2$  m/s<sup>2</sup> for horizontal vibrations.

In the opinion of GRUNDMANN et al. (1993), considering the result of the study of LEONARD (1966), the maximum value of acceleration of vertical vibrations should not exceed the value defined in *Steel, Concrete and Composite...* (1978) and the maximum value of acceleration of horizontal vibrations should not exceed  $1/5$  value of tolerable acceleration of vertical vibrations ( $a_{\max,h} \leq 0.2 a_{\max,v} = 0.1 \cdot f^{0.5}$  m/s<sup>2</sup>).

Different way of evaluation of comfort criteria was presented in *Footbridges – Assessment of vibrational behaviour...* (2006). In these recommendations three levels of comfort (maximum, mean and minimum) were defined. In the case of vertical vibrations maximum comfort is ensured if  $a_{\max,v} \leq 0.5$  m/s<sup>2</sup> (vibrations of the structure are practically imperceptible to the users), average comfort is ensured if  $a_{\max,v} = 0.50\text{--}1.00$  m/s<sup>2</sup> (vibrations of the structure are barely perceptible to the users), minimum comfort is ensured if  $a_{\max,v} = 1.0\text{--}2.5$  m/s<sup>2</sup> (allowed for seldom occurring dynamic loads, accelerations undergone by the structure are perceived by the users, but do not become intolerable). For horizontal vibrations: maximum comfort is ensured if  $a_{\max,h} \leq 0.15$  m/s<sup>2</sup>, average comfort is ensured if  $a_{\max,h} = 0.15\text{--}0.3$  m/s<sup>2</sup>, minimum comfort is ensured if  $a_{\max,h} = 0.3\text{--}0.8$  m/s<sup>2</sup>. Moreover, in the cases of horizontal vibrations when the “lock-in” effect may occur (the effect of synchronization of the pedestrians with the frequency and phase of the horizontal vibrations) in order to avoid the “lock-in” effect the acceleration of the vibrations of the footbridge deck should be limited to  $a_{\max,h} = 0.1$  m/s<sup>2</sup>. The forth range of acceleration of vibrations is also pointed out in the recommendations defining uncomfortable (unacceptable) vibrations. Vibrations with acceleration  $a_{\max,v} \geq 2.5$  m/s<sup>2</sup> are unacceptable in the case of vertical vibrations and vibrations with acceleration  $a_{\max,h} \geq 0.8$  m/s<sup>2</sup> are unacceptable in the case of horizontal vibrations

Furthermore, in *Footbridges – Assessment of vibrational behaviour...* (2006) noted that choice of comfort level is normally influenced by the population using the footbridge and by the level of importance of the structure depending on the location of the footbridge. It is possible to be more demanding on behalf of particularly sensitive users (schoolchildren, elderly or disabled people), and more tolerant in case of short footbridges (short transit times, seldom used footbridge, built to link sparsely populated areas). The footbridge owner should define

the class of the footbridge as a function of the level of traffic intensity and should determine a comfort requirement level to fulfil. Moreover, according to *Footbridges – Assessment of vibrational behaviour...* (2006) in cases of footbridges for which the risk of excitation of resonant vibration is small (when the natural vibration frequencies of the structure are out of the frequency range of human activity i.e. walking, running etc.), comfort level is automatically considered to be ensured.

## Proposal of comfort criteria for footbridges

On the basis of series of in situ experimental investigations performed by Pańtak in 2004–2006 on over 30 footbridges of different structural schemes new proposals of vibration comfort criteria for footbridges were elaborated by Flaga and Pańtak (PAŃTAK 2007, FLAGA, PAŃTAK 2003, 2008). The elaborated proposals are presented in Figure 2.

Proposed comfort criteria taking into account courses of the comfort criteria curves defined in ISO 2636... (1989) and PN-B-02171 (1988) and can be characterized as follows: the criteria are related to the vibrations induced by man, the criteria define the comfort levels in case of vibrations sensed by walking users, the criteria taking into account short duration of stay of the pedestrians on vibrating footbridge, the criteria are related separately to vibrations in vertical and horizontal direction, the criteria are related to peak acceleration ( $a_{\max}$ ) as a function of vibrations frequency, the criteria taking into account frequency of vibrations occurrence: frequent events (base curve M1), rare events (curve M1.7) and exceptional events e.g. vandal actions (curve M10).

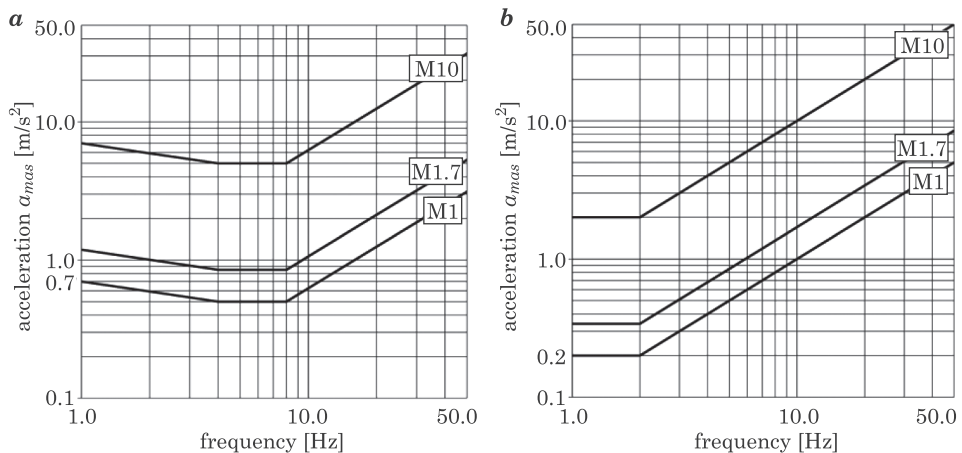


Fig. 2. Proposals of vibration comfort criteria for footbridges:

$a$  – vertical vibrations,  $b$  – horizontal vibrations

Source: based on FLAGA, PAŃTAK (2008).

The base curve M1 for vertical vibrations in frequency range 1.0–8.0 Hz were verified during in situ tests. During the tests, the members of the research team induced the vibrations of the tested footbridges by the rhythmic squats, running or jumping. Pedestrians passing through the footbridge (casual passers-by and other members of the research team) were asked to express their opinion about the vibrations: whether the vibrations were imperceptible or lightly, clearly, very strongly perceptible during the walk, whether the vibrations prevented them from walking and whether they could adjust to vibrations. The vibrations of the structure were acquired using the set of accelerometers. Moreover the time of reaching the vibration measurement point by survey's respondents was measured using stopwatch.

The curve M1 is the base curve corresponding to the following vibration comfort criterion: among surveyed pedestrians walking through the footbridge at most 10% of pedestrians expressed opinion that vibrations were slightly felt or perceptible and did not disturb walking. This curve is proposed in case of frequent event, i.e. vibrations of daily nature occurring once a day or more frequently and not rarely than once a week.

The curve M1.7 is created by multiplying the accelerations defined by curve M1 by multiplier 1.7. Multiplier 1.7 was established to determine the vibrations level at which at least 10% of pedestrians going over the footbridge expressed opinion, that the vibrations were clearly felt (fully perceptible), making slight difficulty in walking or clearly disturb walking. This curve is proposed in case of rare events, i.e. vibrations occurring more rarely than once a week.

The curve M10 is created by multiplying the accelerations defined by curve M1 by multiplier 10. The curve M10 is a curve related to so called vandal intentional actions on a footbridges in a form of e.g. rhythmical jumping on the spot, rhythmical horizontal body movements of a single person or a group of people, rhythmical squats etc. Multiplier 10 was assumed to protect pedestrians against body injuries (mainly legs) caused by vibrations characterised by high acceleration values. It should be emphasized that for the vibrations levels determined by curve M10, comfort of use of the structure is strongly disturbed (free walking is impossible, standing or running is difficult and strongly disturbed).

In the proposed comfort criteria the acceptable value of acceleration of vertical vibrations in frequency range 1.0–4.0 Hz changes from 0.7 m/s<sup>2</sup> to 0.5 m/s<sup>2</sup> according to the equation  $a_{\max,v} = 0.7 \cdot f^{-0.24}$  m/s<sup>2</sup> (where  $f$  in [Hz] is the vibration frequency of the footbridge with high probability of excitation by footbridge users during walking, running, etc. It can be a fundamental or higher vibration frequency of the footbridge). In frequency range 4.0–8.0 Hz the permissible acceleration is constant and equals 0.5 m/s<sup>2</sup>. In the case of vertical vibration with frequency  $f > 8.0$  Hz the comfort criteria were not verified during in situ tests. The acceptable values of acceleration of vertical vibrations were adopted in accordance of the courses of the comfort criteria curves defined

in ISO 2636... (1989) and PN-B-02171 (1988). The course of this comfort curve changes according to the equation  $a_{\max,v} = 0.0625 \cdot f \text{ m/s}^2$  (where  $f$  is as previous).

In the case of horizontal vibrations the base curve M1 was not verified during in situ tests because of lack of the horizontal mode shapes in tested footbridges. The curve M1 for horizontal vibrations was proposed taking into account comfort criteria curves occurring in ISO 2636... (1989) assuming the value of  $a_{\max,h} = 0.2 \text{ m/s}^2$  as the acceptable value of acceleration in frequency range 1.0–2.0 Hz and acceptable acceleration levels  $a_{\max,h} = 0.1f$  for vibrations with frequencies  $f > 2.0 \text{ Hz}$ .

It is worth noting that assessment of the comfort of use of the footbridge using proposed comfort criteria curves is not dependent on the density of the crowd. The proposed comfort criteria curves applies both the assessment of vibrations caused by one person and by a dense crowd. Amplitudes of vibrations must not exceed vibration acceleration levels considered acceptable both during the dynamic action of one person and a dense crowd.

## Comparisons and discussion

Because of many parameters influencing the human sensitivity to vibrations the vibration comfort criteria must represent the average values of permissible vibrations (FLAGA 2002). It should be remembered that characterised comfort criteria proposed by different authors present averaged values of acceptable acceleration of vibrations. It should be also noted that most of these criteria apply to the situations in which vibrations are received by walking persons. Only proposals of ISO 10137... (2007) present the comfort criteria taking into account the footbridge users standing still on the footbridge deck. In the cases of the footbridges located in a place of great cultural, recreational or touristic importance it may be necessary to reduce the vibrations of the structure to values not disturbing standing still users. Despite the opinion of LEONARD (1966) who claimed that it was both uneconomic and unnecessary to design footbridges where standing people will not feel vibrations. Nowadays, such a need arises especially in the case of footbridges designed as a resting places with viewing points and resting regions with places to sit (e.g. benches). The reduction of vibrations of these structure to acceptable values can be realized (if necessary) by means of tuned vibration dampers.

For proper assessment of the comfort of use of the footbridge it is necessary to understand the vibration influence on footbridge users. In Figure 3 the results of research carried out by PAŃTAK (2007) in relation to the comfort criteria proposed by Flaga and Pańtak are presented. This comparison explains the meaning of defined permissible values of acceleration of vibrations.

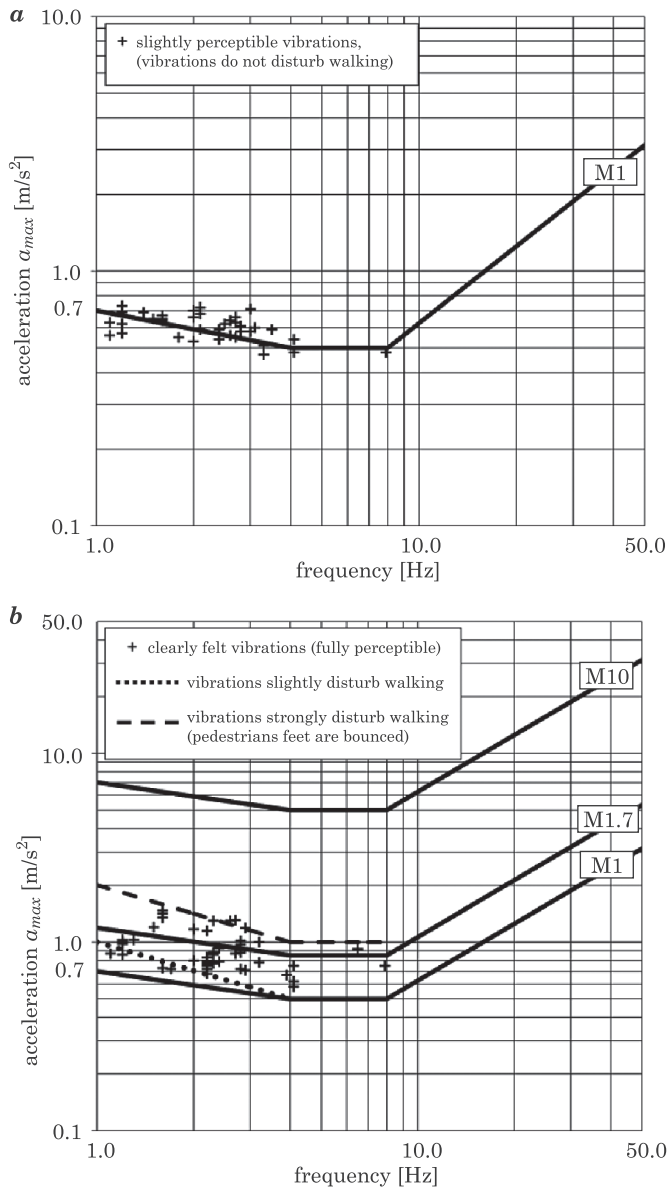


Fig. 3. The comfort criteria proposed by Flaga and Pańtak for vertical vibrations in relation to experimental results: *a* – vibrations slightly perceptible and do not disturbing of walking, *b* – vibrations clearly felt (fully perceptible) and clearly disturbing of walking  
 Source: based on FLAGA, PAŃTAK (2008), PAŃTAK (2007).



It can be seen that in the case of the vertical vibrations the vibrations slightly perceptible and do not disturbing walking are the vibrations with acceleration  $a_{\max,v}=0.5-0.7 \text{ m/s}^2$  (Fig. 3a). Moreover, vibrations with acceleration  $a_{\max,v}=0.7-1.0 \text{ m/s}^2$  are the vibrations clearly felt and slightly disturbing walking. The vibrations with acceleration  $a_{\max,v} > 1.0 \text{ m/s}^2$  are clearly felt and clearly disturbing walking (pedestrians feet are bounced off the footbridge deck). In the case of  $a_{\max,v} > 1.5 \text{ m/s}^2$  the vibrations are unpleasant and walking is strongly disturbed.

Having regard to the above conclusions it is possible to assess the comfort criteria presented in all standards and recommendations cited in the paper.

Evaluating the recommendations presented in ISO 10137... (2007) it is important to remember that the comfort criteria presented in ISO 10137... (2007) are defined in terms of root-mean-square (*rms*) value of acceleration. To compare the criteria ISO 10137... (2007) with other recommendations the value of acceleration  $a_{rms}$  need to be converted to the peak value  $a_{\max}$ , proper for harmonic vibrations, by multiplying values of  $a_{rms}$  by the factor  $\sqrt{2}$ . In Figure 4 the comparisons of the comfort criteria ISO 10137... (2007) converted to peak acceleration  $a_{\max}$  with the criteria proposed by FLAGA and PAŃTAK (2008) are presented.

It can be seen that in the case of vertical vibration both base curve M1 and curve (ISO 10137... 2007) with multiplier 60 (converted to  $a_{\max}$ ) define the similar values of permissible peak acceleration of vibrations. In the case of horizontal vibrations the ISO 10137... (2007) curve (converted to  $a_{\max}$ ) is located much higher than base curve M1 proposed by FLAGA and PAŃTAK (2008). Comparison of the requirement of ISO 10137... (2007) for horizontal vibrations with recommendations of other author ( $a_{\max,h}=0.1-0.2 \text{ m/s}^2$ ) also indicate that requirement of ISO 10137... (2007) is gentler and probably should be verified. Using multiplier from the range 20 to 40 instead of 60 recommended in ISO 10137... (2007) allows to achieve the value of permissible acceleration of the horizontal vibrations  $a_{\max,h}=0.1-0.2 \text{ m/s}^2$ .

The limit values of the vertical vibrations acceleration assumed in the comfort criteria proposed by FLAGA and PAŃTAK (2008) correspond to the comfort threshold for vibrations sensed by walking users. For standing users permissible values of vibrations accelerations are lower and can be determined using a reduction factor 0.30–0.35 for the M1 curve.

The comfort criteria defined in *Footbridges – Assessment of vibrational behaviour...* (2006) present a comprehensive approach to assessment of the comfort of use of the vibrating footbridges. The three levels of comfort of use of the footbridge defined in recommendations together with additional assessment of importance of the structure depending on its location and traffic intensity allow to assume appropriate comfort criterion by the designer and the owner of the footbridge. The levels of vibrations acceleration defined in *Footbridges – Assessment of vibrational behaviour...* (2006) recommendations for maximum



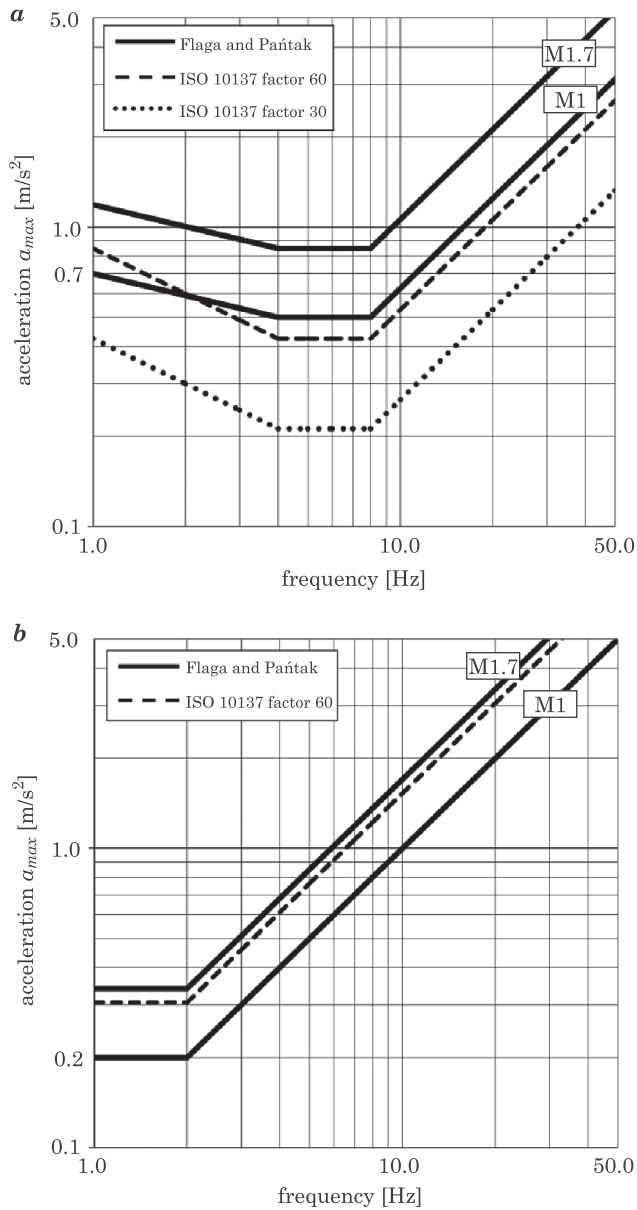


Fig. 4. Comparison of comfort criteria (dotted and dashed lines) converted to peak acceleration of vibrations  $a_{max}$  with criteria proposed by Flaga and Paňtak (solid bold line marked with M1 and M1.7 tags): *a* – vertical vibrations, *b* – horizontal vibrations  
Source: based on ISO 10137... (2007), PAŇTAK (2007), FLAGA, PAŇTAK (2008).

and mean comfort are in line with the proposals of other authors. In the case of minimum comfort the upper bound of acceleration of vertical vibrations seems to be too high ( $a_{\max,v} = 2.5 \text{ m/s}^2$ ). Although this large value of acceleration of vibrations according to *Footbridges – Assessment of vibrational behavior...* (2006) is allowed only in the case of seldom occurring vibrations it is important to remember that vibrations with  $a_{\max,v} > 1.5 \text{ m/s}^2$  are unpleasant and walking is strongly disturbed (PAŃTAK 2007).

The comfort criteria recommended by *Steel, Concrete and Composite...* (1978), BACHMANN, AMMANN (1987), GRUNDMANN et. al. (1993) are appropriate recommendations in frequency range of 1.0–8.0 Hz for vertical vibrations and 1.0–2.0 Hz for horizontal vibrations. Nevertheless a more accurate determination of the permissible value of acceleration of vibrations for a given frequency of vibration is possible using comfort criteria defined in ISO 10137... (2007) or by FLAGA and PAŃTAK (2008).

In the light of the above considerations the comfort criteria presented in PN-EN 1990:2004/A1 (2008) can be considered as a simply rules for preliminary assessment of the comfort of use of the vibrating footbridges. It should be noted that in the case of vertical vibrations of the footbridge deck with frequency  $f > 1.0 \text{ Hz}$  the vibrations of the structure reaching the value of acceleration of vibrations  $a_{\max,v} = 0.7 \text{ m/s}^2$  will be slightly perceptible by the users. The value of permissible acceleration  $a_{\max,v} = 0.7 \text{ m/s}^2$  recommended in PN-EN 1990:2004/A1 (2008) is in the range of the medium (mean) comfort of use of the structure defined in *Footbridges – Assessment of vibrational behaviour...* (2006). The requirements for horizontal vibrations defined in PN-EN 1990:2004/A1 (2008) are in good agreement with numerous recommendations of other authors.

More comprehensive methodology of assessment of the comfort of use of the footbridges taking into account frequency of vibrations occurrence (frequent events, rare events, exceptional events) and different levels of comfort of use in a function of location of the footbridge and forecasted traffic intensity seems to be appropriate and should be elaborated in National Annex of the standard PN-EN 1990:2004/A1 (2008). It is important to elaborate and consider in analyses the comfort criteria taking into account the probability of occurrence of resonant vibrations in a function of location of the footbridge (compare recommendations presented in *Footbridges – Assessment of vibrational behaviour...* (2006). Occurrence of some type of vibration excitation on footbridges can be unlikely in different locations as well as occurrence of footbridge vibrations can be acceptable or unacceptable depending on its location. For example: vibration with a maximum acceleration amplitude e.g.  $1.5 \text{ m/s}^2$  (i.e. vibrations clearly disturbing walking) excited by e.g. twelve jumping people can be considered as unlikely and generated vibrations can be acknowledged as acceptable even in the case of footbridge located in the busy city centre due to their rare occurrence, while the same vibration with a maximum amplitude  $1.5 \text{ m/s}^2$  excited by one jumping person should be considered

as a case characterized by a high probability of occurrence and unacceptable in the case of footbridge located in the busy city centre but acceptable in the case of footbridge located in the rural area due to their rare occurrence. The influence of the location of the footbridge on the comfort criteria is an important issue and requires further research and analyses. Nevertheless it should be remembered that assessment of the comfort of use of the footbridges performed on the basis of the results obtained for resonant excitations without knowing the probability of occurrence of the resonance effects during the everyday operation of the structure is an irrational and incorrect procedure.

It should be also noted that all comfort criteria characterised in this paper do not present a proposal of acceptable level of acceleration for running users and cyclists. The runners are less sensitive to vibrations than walking pedestrians (in other words evaluation of comfort of use of the footbridge during vibrations sensed by walking users is more severe restriction) but in some cases evaluation of the comfort of use of the footbridges during vibrations induced and sensed by running users can be important (e.g. occasional sport events, marathons etc.).

The next important and particular type of the footbridges users are the cyclists. The cyclists are the next type of “vibration receiver”. They receiving the vibrations in particular way. They sitting on a bicycle saddle and receiving vibrations through the hands, feet and buttocks. Because of that the cyclists become more sensitive to vibrations. It can be important to assess the comfort of use of the structure by cyclists especially in cases of long span footbridges located in popular recreational areas and used by cyclists, pedestrians and runners.

## Summary

Comfort of use of the footbridges is a serious problem in case of slender and lightweight structures. The vibrations are important limit state in footbridges design. Dynamic analysis is indispensable step in the design of modern footbridges. Static analyses are insufficient to verify all important requirements of serviceability limit state.

To assess the comfort of use of the footbridges it is important both to know the acceptable value of acceleration of vibrations as well as the frequency of occurrence of the vibrations. It is advisable to specify and take into account the different levels of comfort of use of the footbridges and consider the importance of the structure depending on the place of its location. It seems important to elaborate the methodology of assessment of the comfort of use of the footbridges taking into account the probability of occurrence of the resonant excitation for different types of dynamic impact (walking, running, jumping, squats etc.) and different frequencies of excitation of the vibrations in a function of location of the footbridge.

## References

- BACHMANN H., AMMANN W. 1987. *Vibration in structures induced by man and machine*. International Association of Bridge and Structural Engineering (IABSE), Zurich.
- FLAGA A. 2002. *Problems of vibrations effects on people on bridges*. Inżynieria i Budownictwo, 3–4: 182–187.
- FLAGA A., PAŃTAK M. 2003. *The Comfort criteria in the design of footbridges*. Proc. of Sem. Design, construction and aesthetics of pedestrian bridges, Cracow University of Technology, p. 7–27.
- FLAGA A., PAŃTAK M. 2008. *Vibration comfort criteria for pedestrians on footbridges*. Proc. Third Inter. Conf. Footbridges, Faculdade de Engenharia Universidade do Porto, Porto.
- Footbridges – Assessment of vibrational behaviour of footbridges under pedestrian loading – Practical Guidelines*. 2006. Technical Department for Transport, Roads and Bridges Engineering and Road Safety (Service d'études techniques des routes et autoroutes – SÉTRA), Paris.
- GRUNDMANN H., KREUZINGER H., SCHNEIDER M. 1993. *Schwingungsuntersuchungen für Fußgängerbrücken*. Springer-Verlag, Bauingenieur, 68: 215–225.
- ISO 10137:2007. *Bases for Design of Structures. Serviceability of buildings and walkways against vibrations*. 2007. International Organization for Standardization, Geneva.
- ISO 2631:2–1989. *Mechanical vibration and shock. Evaluation of human exposure to whole-body vibration. Part 2. Continuous and shock-induced vibration in buildings (1 to 80 Hz)*. 1989. International Standardization Organization, Geneva.
- LEONARD D.R. 1966. *Human tolerance levels for bridge vibrations*. RRL, Report No. 34, Harmondsworth.
- PAŃTAK M. 2007. *Analysis of vibration comfort criteria for steel footbridges susceptible to dynamic actions*. PhD Thesis, Cracow University of Technology, Cracow.
- PAŃTAK M. 2012. *Application of EN 1990/A1 vibration serviceability limit state requirements for steel footbridges*. Procedia Engineering, 40: 345 – 350.
- PN-B-02171. *Evaluation of the impact of vibrations on people in buildings*. 1988. PKN, Warszawa.
- PN-EN 1990:2004/A1. *Eurocode – Basis of structural design*. 2008. Chapter A2.4. PKN, Warszawa.
- PN-EN 1991-2:2007. *Eurocode 1: Actions on structures. Part 2. Traffic loads on bridges*. 2007. Chapter 5.1(4). PKN, Warszawa.
- Steel, Concrete and Composite Bridges. Part 2. Specification for Loads*. 1978. BS 5400-2:1978. British Standards Association, London.

## **Guide for Authors**

### **Introduction**

Technical Sciences is a peer-reviewed research Journal published in English by the Publishing House of the University of Warmia and Mazury in Olsztyn (Poland). Journal is published continually since 1998. Until 2010 Journal was published as a yearbook, in 2011 and 2012 it was published semiyearly. From 2013, the Journal is published quarterly in the spring, summer, fall, and winter.

The Journal covers basic and applied researches in the field of engineering and the physical sciences that represent advances in understanding or modeling of the performance of technical and/or biological systems. The Journal covers most branches of engineering science including biosystems engineering, civil engineering, environmental engineering, food engineering, geodesy and cartography, information technology, mechanical engineering, materials science, production engineering etc.

Papers may report the results of experiments, theoretical analyses, design of machines and mechanization systems, processes or processing methods, new materials, new measurements methods or new ideas in information technology.

The submitted manuscripts should have clear science content in methodology, results and discussion. Appropriate scientific and statistically sound experimental designs must be included in methodology and statistics must be employed in analyzing data to discuss the impact of test variables. Moreover there should be clear evidence provided on how the given results advance the area of engineering science. Mere confirmation of existing published data is not acceptable. Manuscripts should present results of completed works.

There are three types of papers: a) research papers (full length articles); b) short communications; c) review papers.

The Journal is published in the printed and electronic version. The electronic version is published on the website ahead of printed version of Technical Sciences.

**Technical Sciences does not charge submission or page fees.**

### **Types of paper**

The following articles are accepted for publication:

#### **Reviews**

Reviews should present a focused aspect on a topic of current interest in the area of biosystems engineering, civil engineering, environmental engineering, food engineering, geodesy and cartography, information technology, mechanical engineering, materials science, production engineering etc. They should include all major findings and bring together reports from a number of sources. These critical reviews should draw out comparisons and conflicts between work, and provide an overview of the 'state of the art'. They should give objective assessments of the topic by citing relevant published work, and not merely present the opinions of individual authors or summarize only work carried out by the authors or by those with whom the authors agree. Undue speculations should also be avoided. Reviews generally should not exceed 6,000 words.

#### **Research Papers**

Research Papers are reports of complete, scientifically sound, original research which contributes new knowledge to its field. Papers should not exceed 5,000 words, including figures and tables.

### **Short Communications**

Short Communications are research papers constituting a concise description of a limited investigation. They should be completely documented, both by reference list, and description of the experimental procedures. Short Communications should not occupy more than 2,000 words, including figures and tables.

### **Letters to the Editor**

Letters to the Editor should concern with issues raised by articles recently published in scientific journals or by recent developments in the engineering area.

### **Contact details for submission**

The paper should be sent to the Editorial Office, as a Microsoft Word file, by e-mail: techsci@uwm.edu.pl

### **Referees**

Author/authors should suggest, the names, addresses and e-mail addresses of at least three potential referees. The editor retains the sole right to decide whether or not the suggested reviewers are used.

### **Submission declaration**

After final acceptance of the manuscript, the corresponding author should send to the Editorial Office the author's declaration. Submission of an article implies that the work has not been published previously (except in the form of an abstract or as part of a published lecture or academic thesis or as an electronic preprint), that it is not under consideration for publication elsewhere, that publication is approved by all authors and tacitly or explicitly by the responsible authorities where the work was carried out, and that, if accepted, it will not be published elsewhere in the same form, in English or in any other language.

To prevent cases of ghostwriting and guest authorship, the author/authors of manuscripts is/are obliged to: (i) disclose the input of each author to the text (specifying their affiliations and contributions, i.e. who is the author of the concept, assumptions, methods, protocol, etc. used during the preparation of the text); (ii) disclose information about the funding sources for the article, the contribution of research institutions, associations and other entities.

### **Language**

Authors should prepare the full manuscript i.e. title, abstract and the main text in English (American or British usage is accepted). Polish version of the manuscript is not required.

### **The file type**

Text should be prepared in a word processor and saved in doc or docx file (MS Office).

### **Article structure**

Suggested structure of the manuscript is as follows:

Title

Authors and affiliations

Corresponding author

Abstract

Keywords

Introduction

Material and Methods

Results and Discussion

Conclusions

Acknowledgements (optional)  
References  
Tables  
Figures

### **Subdivision – numbered sections**

Text should be organized into clearly defined and numbered sections and subsections (optionally). Sections and subsections should be numbered as 1. 2. 3. then 1.1 1.2 1.3 (then 1.1.1, 1.1.2, ...). The abstract should not be included in numbering section. A brief heading may be given to any subsection. Each heading should appear on its own separate line. A single line should separate paragraphs. Indentation should be used in each paragraph.

Font guidelines are as follows:

- Title: 14 pt. Times New Roman, bold, centered, with caps
- Author names and affiliations: 12 pt. Times New Roman, bold, centered, italic, two blank line above
- Abstract: 10 pt. Times New Roman, full justified, one and a half space. Abstract should begin with the word Abstract immediately following the title block with one blank line in between. The word Abstract: 10 pt. Times New Roman, centered, indentation should be used
- Section Headings: Not numbered, 12 pt. Times New Roman, bold, centered; one blank line above
- Section Sub-headings: Numbered, 12 pt. Times New Roman, bold, italic, centered; one blank line above
- Regular text: 12 pt. Times New Roman, one and a half space, full justified, indentation should be used in each paragraph

### **Title page information**

The following information should be placed at the first page:

#### **Title**

Concise and informative. If possible, authors should not use abbreviations and formulae.

#### **Authors and affiliations**

Author/authors' names should be presented below the title. The authors' affiliation addresses (department or college; university or company; city, state and zip code, country) should be placed below the names. Authors with the same affiliation must be grouped together on the same line with affiliation information following in a single block. Authors should indicate all affiliations with a lower-case superscript letter immediately after the author's name and in front of the appropriate address.

#### **Corresponding author**

It should be clearly indicated who will handle correspondence at all stages of refereeing and publication, also post-publication process. The e-mail address should be provided (footer, first page). Contact details must be kept up to date by the corresponding author.

#### **Abstract**

The abstract should have up to 100-150 words in length. A concise abstract is required. The abstract should state briefly the aim of the research, the principal results and major conclusions. Abstract must be able to stand alone. Only abbreviations firmly established in the field may be eligible. Non-standard or uncommon abbreviations should be avoided, but if essential they must be defined at their first mention in the abstract itself.

## **Keywords**

Immediately after the abstract, author/authors should provide a maximum of 6 keywords avoiding general, plural terms and multiple concepts (avoid, for example, 'and', 'of'). Author/authors should be sparing with abbreviations: only abbreviations firmly established in the field may be eligible.

## **Abbreviations**

Author/authors should define abbreviations that are not standard in this field. Abbreviations must be defined at their first mention there. Author/authors should ensure consistency of abbreviations throughout the article.

## **Units**

All units used in the paper should be consistent with the SI system of measurement. If other units are mentioned, author/authors should give their equivalent in SI.

## **Introduction**

Literature sources should be appropriately selected and cited. A literature review should discuss published information in a particular subject area. Introduction should identify, describe and analyze related research that has already been done and summarize the state of art in the topic area. Author/authors should state clearly the objectives of the work and provide an adequate background.

## **Material and Methods**

Author/authors should provide sufficient details to allow the work to be reproduced by other researchers. Methods already published should be indicated by a reference. A theory should extend, not repeat, the background to the article already dealt within the Introduction and lay the foundation for further work. Calculations should represent a practical development from a theoretical basis.

## **Results and Discussion**

Results should be clear and concise. Discussion should explore the significance of the results of the work, not repeat them. A combined Results and Discussion section is often appropriate.

## **Conclusions**

The main conclusions of the study may be presented in a Conclusions section, which may stand alone or form a subsection of a Results and Discussion section.

## **Acknowledgements**

Author/authors should include acknowledgements in a separate section at the end of the manuscript before the references. Author/authors should not include them on the title page, as a footnote to the title or otherwise. Individuals who provided help during the research study should be listed in this section.

## **Artwork**

### **General points**

- Make sure you use uniform lettering and sizing of your original artwork
- Embed the used fonts if the application provides that option
- Aim to use the following fonts in your illustrations: Arial, Courier, Times New Roman, Symbol
- Number equations, tables and figures according to their sequence in the text
- Size the illustrations close to the desired dimensions of the printed version



## **Formats**

If your electronic artwork is created in a Microsoft Office application (Word, PowerPoint, Excel) then please supply 'as is' in the native document format

Regardless of the application used other than Microsoft Office, when your electronic artwork is finalized, please 'Save as' or convert the images to one of the following formats (note the resolution requirements given below):

EPS (or PDF): Vector drawings, embed all used fonts

JPEG: Color or grayscale photographs (halftones), keep to a minimum of 300 dpi

JPEG: Bitmapped (pure black & white pixels) line drawings, keep to a minimum of 1000 dpi or combinations bitmapped line/half-tone (color or grayscale), keep to a minimum of 500 dpi

### **Please do not:**

- Supply files that are optimized for screen use (e.g., GIF, BMP, PICT, WPG); these typically have a low number of pixels and limited set of colors
- Supply files that are too low in resolution
- Submit graphics that are disproportionately large for the content

## **Color artwork**

Author/authors should make sure that artwork files are in an acceptable format (JPEG, EPS PDF, or MS Office files) and with the correct resolution. If, together with manuscript, author/authors submit color figures then Technical Sciences will ensure that these figures will appear in color on the web as well as in the printed version at no additional charge.

## **Tables, figures, and equations**

Tables, figures, and equations/formulae should be identified and numbered consecutively in accordance with their appearance in the text.

Equations/mathematical and physical formulae should be presented in the main text, while tables and figures should be presented at the end of file (after References section). Mathematical and physical formulae should be presented in the MS Word formula editor.

All types of figures can be black/white or color. Author/authors should ensure that each figure is numbered and has a caption. A caption should be placed below the figure. Figure must be able to stand alone (explanation of all symbols and abbreviations used in figure is required). Units must be always included. It is noted that figure and table numbering should be independent.

Tables should be numbered consecutively in accordance with their appearance in the text. Table caption should be placed above the table. Footnotes to tables should be placed below the table body and indicated with superscript lowercase letters. Vertical rules should be avoided. Author/authors should ensure that the data presented in tables do not duplicate results described in figures, diagrams, schemes, etc. Table must be able to stand alone (explanation of all symbols and abbreviations used in table is required). Units must be always included. As above, figure and table numbering should be independent.

## **References**

References: All publications cited in the text should be presented in a list of references following the text of the manuscript. The manuscript should be carefully checked to ensure that the spelling of authors' names and dates of publications are exactly the same in the text as in the reference list. Authors should ensure that each reference cited in the text is also present in the reference list (and vice versa).

Citations may be made directly (or parenthetically). All citations in the text should refer to:

1. Single author

The author's name (without initials, with caps, unless there is ambiguity) and the year of publication should appear in the text

2. Two authors

Both authors' names (without initials, with caps) and the year of publication should appear in the text

3. Three or more authors

First author's name followed by et al. and the year of publication should appear in the text

Groups of references should be listed first alphabetically, then chronologically.

*Examples:*

"... have been reported recently (ALLAN, 1996a, 1996b, 1999; ALLAN and JONES, 1995). KRAMER et al. (2000) have recently shown..."

The list of references should be arranged alphabetically by authors' names, then further sorted chronologically if necessary. More than once reference from the same author(s) in the same year must be identified by the letters "a", "b", "c" etc., placed after the year of publication.

References should be given in the following form:

KUMBHAR B.K., AGARVAL R.S., DAS K. 1981. Thermal properties of fresh and frozen fish. *International Journal of Refrigeration*, 4(3), 143–146.

MACHADO M.F., OLIVEIRA F.A.R., GEKAS V. 1997. Modelling water uptake and soluble solids losses by puffed breakfast cereal immersed in water or milk. In *Proceedings of the Seventh International Congress on Engineering and Food*, Brighton, UK.

NETER J., KUTNER M.H., NACHTSCHEIM C.J., WASSERMAN W. 1966. *Applied linear statistical models* (4th ed., pp. 1289–1293). Irwin, Chicago.

THOMSON F.M. 1984. Storage of particulate solids. In M. E. Fayed, L. Otten (Eds.), *Handbook of Powder Science and Technology* (pp. 365–463). Van Nostrand Reinhold, New York.

Citation of a reference as 'in press' implies that the item has been accepted for publication.

Note that the full names of Journals should appear in reference list.

### **Submission checklist**

The following list will be useful during the final checking of an article prior to the submission. Before sending the manuscript to the Journal for review, author/authors should ensure that the following items are present:

- Text is prepared with a word processor and saved in DOC or DOCX file (MS Office).
- One author has been designated as the corresponding author with contact details: e-mail address
- Manuscript has been 'spell-checked' and 'grammar-checked'
- References are in the correct format for this Journal
- All references mentioned in the Reference list are cited in the text, and vice versa
- Author/authors does/do not supply files that are too low in resolution
- Author/authors does/do not submit graphics that are disproportionately large for the content